Aus der V. Medizinischen Klinik: Nephrologie, Endokrinologie und Rheumatologie
der Medizinischen Fakultät Mannheim
Direktor: Prof. Dr. med. B. Krämer

Enzyme-triggered CO-releasing molecules (ET-CORMs): towards tissue-specific delivery of carbon monoxide

Inauguraldissertation
zur Erlangung des medizinischen Doktorgrades
der
Medizinischen Fakultät Mannheim
der Ruprecht-Karls-Universität
zu
Heidelberg

vorgelegt von
Dennis Storz

aus
Villingen-Schwenningen

2018

Dean:	Prof. Dr. med. Sergij Goerdt
Supervisor:	Prof. Dr. rer. nat. Benito A. Yard

Meinen Eltern.

Contents

Abbreviations

APS	Ammonium persulfate
ARE	Antioxidant response element
ATP	Adenosine triphosphate
°C	Degrees Celsius
$CD4^+$	Cluster of Differentiation 4
CO	Carbon monoxide
CO_2	Carbon dioxide
COP-1	CO Probe 1
COX	Cytochrome c oxidase
ddH_2O	Double distilled water
DEPC	Diethylpyrocarbonate
DFO	Deferoxamine
dH_2O	distilled water
DMSO	Dimethyl sulfoxide
(c)DNA	(complementary) Deoxyribonucleic acid
DPD	2,2'-dipyridyl
DTT	1,4-Dithio-DL-treithol
ECL	Enhanced Chemi Luminescence
EDTA	Ethylenediaminetetraacetic acid
ET-CORM	Enzyme-triggered CO-releasing molecule
$FeCl_2$	Ferrous chloride
$FeCl_3$	Ferric chloride
FCS	Fetal calf serum
FumET-CORM	Methyl fumarate-derived compounds
GAPDH	Glyceraldehyde 3-phosphate dehydrogenase
cGMP	cyclic guanosine monophosphate
GSH	Glutathione
h	Hours
^3H	Tritium
H_2S	Hydrogen sulfide
HCl	Hydrochloric acid
HO-1	Haem oxygenase 1
HRP	Horseradish peroxidase
HUVEC	Human umbilical vein endothelial cells

IκBα	Nuclear factor of kappa light polypeptide gene enhancer in B-cells inhibitor, alpha
IKK	IκB kinase
IMDM	Iscove's Modified Dulbecco's Medium
IRP	Iron regulatory protein
kDa	Kilo Dalton
Keap1	Kelch-like ECH-associated protein 1
L	Liter
LCI	Labile cell iron
LIP	Labile iron pool
LDH	Lactate dehydrogenase
µg	Microgram
µl	Microliter
µM	Micromolar
µm	Micrometer
mA	Milliampere
min	Minutes
mg	Milligram
ml	Milliliter
mM	Millimolar
MTT	3-(4,5-dimethylthiazol-2-yl)-2,5-diphenyl tetrazolium bromide
mV	Millivolt
NaCl	Sodium chloride
NfκB	Nuclear factor kappa-light-chain enhancer of activated B-cells
ng	Nano gram
nm	Nano meter
NO	Nitric oxide
NOS	Nitric oxide synthase
iNOS	Inducible Nitric oxide synthase
Nrf2	Nuclear factor (erythroid-derived) 2-related factor 2
OCORS	Oral Carbon Monoxide Release System
OD	Optical density
qPCR	quantitative Polymerase chain reaction
PBMC	Peripheral blood mononuclear cell
PBS	Phosphate-buffered saline
PGA	Penicillin G amidase
PTEC	Proximal tubular epithelial cells

rcf	relative centrifugal force
RNA	Ribonucleic acid
ROI	Reactive oxygen intermediates
ROS	Reactive oxygen species
rpm	Rotation per minute
RT	Room temperature
SD	Standard deviation
SDS	Sodium dodecyl sulfate
SDS-PAGE	Sodium dodecyl sulfate – polyacrylamide gel electrophoresis
TBS	Tris buffered saline
TEMED	Tetramethylethylenediamine
TNF-α	Tumour necrosis factor alpha
UV light	Ultraviolet light
VCAM-1	Vascular cell adhesion molecule 1
WB	Western blot

1 Introduction

1.1 Gasotransmitter: An efficient family of messenger molecules

Gasotransmitter represent a class of gaseous molecules that are endogenously generated and involved in a variety of cell signaling mechanisms [Wang, 2014]. In contrast to classic messenger molecules, e.g., neurotransmitters or hormones [Mustafa et al., 2009], gasotransmitters benefit from their membrane permeability and fast diffusion properties. Due to these properties gasotransmitters are present in all organs where they affect cell metabolism in a more immediate manner. Recent research has illuminated the potential of gasotransmitters and the significance of their signaling network [Mann and Motterlini, 2007]. This has opened up new avenues and perspectives of these molecules and paved the way for possible clinical applications. NO, CO and H_2S, are currently forming the family of gasotransmitters, as these molecules share common features and fulfill the criteria for being a gasotransmitter [Wang, 2002, 2014]. They all share commonalities in terms of reaction with haemoglobin, inhibition of cellular respiration presumably via cytochrome c oxidase, vasodilatation and modulation of inflammatory responses. However, the signaling mechanisms and pathways of each of the gasotransmitters vary in many aspects [Szabo, 2007].

1.1.1 Nitric oxide

NO was the first identified gaseous signaling molecule [Wang, 2014], long before the term 'gasotransmitter' was introduced in the year 2002 [Wang, 2002]. First declared as noxious, nitric oxide is now considered an essential molecule in living organisms as research in this field progressed [Alberto and Motterlini, 2007]. NO is endogenously generated by the enzyme NO synthase (NOS) using L-arginine as the main substrate. There are three isoforms of this enzyme, the most significant being the widespread inducible NO synthase (iNOS). The dominant biological effect of nitric oxide is activation of soluble guanylyl cyclase (sGC) leading to the generation of cGMP, which subsequently feeds a variety of signaling pathways. The plethora of biological effects conveyed by NO includes relaxation of smooth muscle cells, inhibition of smooth muscle cell growth, and preventing of platelet aggregation [McDonald and Murad, 1996; Moncada and Higgs, 1991; Moncada et al., 1991; Murad, 1994]. Unveiling of these biological properties unquestionably contributed to the design and implementation of NO based pharmaceuticals, today used in the acute treatment of angina pectoris (glyceryl trinitrate) or hypertensive emergency

(sodium nitroprusside). To underline the importance of the gasotransmitter nitric oxide, the scientists who described the physiological function of NO were awarded the Nobel Prize in Medicine 1998.

1.1.2 Hydrogen sulfide

The latest member of the gasotransmitter family is H_2S [Wang, 2002]. This gaseous molecule is endogenously produced in various mammalian cells by cystathionine β-synthase and cystathionine γ-lyase from the substrate L-cysteine. These enzymes are mainly expressed in the nervous system, liver, kidney and smooth muscle cells [Szabo, 2007]. Previously published *in vivo* data indicates that H_2S might have beneficial effects in terms of cytoprotection [Pan et al., 2006], adhesion of neutrophils [Fiorucci et al., 2005; Zanardo et al., 2006], modulation of inflammatory response [Sodha et al., 2009; Sodha and Sellke, 2015] and myocardial ischemia-reperfusion [Johansen et al., 2006].
More recently, growing interest evolved in the research of H_2S [Wang, 2014], including the design of H_2S-releasing compounds [Powell et al., 2018]. Interestingly, an intravenous H_2S-related compound entered a phase I trial for safety and tolerability [Szabo, 2007; Toombs et al., 2010], although an intended phase II trial was terminated. There is still a need to further evaluate the biological effects and signaling mechanisms since H_2S can be very noxious at higher concentrations [Szabo, 2007].

1.1.3 Carbon monoxide: Poisonous yet promising?

The third member of the group of gasotransmitter is carbon monoxide, which is endogenously produced during physiological degradation of haem in mammalian cells [Rochette et al., 2013]. Responsible for the catabolism of haem are haem oxygenase (HO) enzymes [Sjostrand, 1951, 1952b], which cleave haem to biliverdin, carbon monoxide and ferrous iron (Fe^{2+}) [Bauer and Pannen, 2009; Coburn, 1970; Coburn et al., 1963; Sjostrand, 1952a; Tenhunen et al., 1968]. Subsequently, the ferrous iron is sequestered by ferritin until further usage. Biliverdin is converted by biliverdin reductase into bilirubin, which is then excreted. The released carbon monoxide has a high affinity for haem-containing proteins, both intracellular and extracellular. Ultimately, CO diffuses, binds to haemoglobin and is exhaled through the lungs.
In a homeostatic state, the colorless and odorless gas is generated only in small amounts [Gullotta et al., 2012]. The physiological production of CO can be quantified at a rate of about 16 µmol/h per human body [Heinemann et al., 2014]. In comparison to NO, carbon monoxide is inert and has a much longer half-life [Johnson et al., 1999; Rochette et al., 2013]. NO is highly reactive in oxidative conditions leading to formation of peroxynitrite, which may aggravate inflammatory and oxidative stress [Pacher et al., 2007; Wagener et al., 2003],
At elevated concentrations, however, CO is considered to be highly toxic to living organisms. This intoxication is mainly caused by (prolonged) exposure to environmentally generated, exogenous CO [Wu and Wang, 2005]. Compared to O_2, carbon monoxide has a 200-times higher affinity to bind to haemoglobin. The resulting carboxyhaemoglobin diminishes the blood capacity to transport oxygen [Heinemann et al., 2014]. Interestingly, this may not be the major cause for the toxicity of CO in living organisms. The toxic effect is most likely the increase of intracellular CO concentration and tissue accumulation, leading to disturbance of mitochondrial function and impairment of cellular respiration [Schatzschneider, 2015].

Despite the noxious effect of high amounts of carbon monoxide, low concentrations of CO mediate essential physiological functions. This ambivalence of CO was demonstrated for the first time by data published by Marks *et al.* and others, that showed vasodilatative effects for endogenous carbon monoxide [Marks et al., 1991; Motterlini et al., 1998; Suematsu et al., 1995, 1994; Wang et al., 1997]. In recent years, the ambiguous property of CO as a key factor in cellular physiology and pathophysiology has been further delineated, as biological effects mediated by endogenous CO can be mimicked by application of the exogenous equivalents. However, the research of CO lags approximately 25 years behind when compared to NO [Mann and Motterlini, 2007].

1.2 The haem oxygenase system

In the catabolism of haem and endogenous production of CO, haem oxygenases are the rate-limiting enzymes [Wagener et al., 2003]. These enzymes are highly conserved [Wagener et al., 2003], and consist of three isoforms [Maines, 1997; McCoubrey et al., 1997]. HO-2 and HO-3 are constitutively expressed, whereas HO-1 is the inducible isoform, the expression of which differs highly in different cell types [Morse and Choi, 2002]. Haem oxygenase-1 is mainly upregulated under oxidative conditions or by redox active agents [Applegate et al., 1991; Otterbein et al., 2000; Otterbein and Choi, 2000]. Previous studies identified various beneficial characteristics for HO-1 in terms of cytoprotection and apoptosis [Inguaggiato et al., 2001; Otterbein et al., 1999; Yang et al., 1999] as well as immunomodulation [Ke et al., 2002]. The beneficial properties of HO-1 during oxidative stress and inflammation are believed to be mediated via the byproducts of haem degradation, i.e., CO and bilirubin [Mustafa et al., 2009; Ryter and Choi, 2009].

1.3 Application of exogenous carbon monoxide

Initially CO has been used for *in vitro* and *in vivo* studies mainly in its gaseous form, i.e., either by CO inhalation or by making use of CO gassed buffer solutions.
In vitro, carbon monoxide demonstrates cytoprotective and anti-proliferative properties [Brouard et al., 2000; Sarady et al., 2002]. In terms of inflammation, CO appears to diminish pro-inflammatory cytokines and to induce anti-inflammatory cytokines [Otterbein et al., 2000]. CO-enriched preservation solution seems to inhibit intimal hyperplasia [Nakao et al., 2011] and reduces reperfusion injury for lung grafts [Kohmoto et al., 2008], the intestines [Nakao et al., 2006] and kidney grafts [Nakao et al., 2008] of rats.
The administration of CO via inhalation has been extensively explored *in vivo*. In this concept, delivery of CO to tissues occurs via the formation of carboxyhaemoglobin. Various studies have demonstrated the therapeutic potential of this approach in a variety of models. Inhalation of CO alleviates symptoms of pulmonary hypertension in mice [Zuckerbraun et al., 2006]. In rat models, CO ameliorates reperfusion injury in kidney [Neto et al., 2004], lung [Kohmoto et al., 2006; Song et al., 2003] and heart [Nakao et al., 2010]. Beneficial effects of CO inhalation were also shown in cardiac transplantation models and arteriosclerosis [Otterbein et al., 2003b; Sato et al., 2001], possibly mediated via modulation of cytokine expression resulting in anti-inflammatory effects [Otterbein et al., 2000].
Several clinical trials administering CO via inhalation are currently ongoing (www.clinicaltrials.gov, #NCT02425579, #NCT00094406). Phase II clinical studies showed safe application of low

dose CO inhalation and beneficial trends in patients with stable COPD [Bathoorn et al., 2007] and in patients with idiopathic pulmonary fibrosis [Rosas et al., 2018], however no significance was accomplished.
It is expected that in humans high concentrations of carbon monoxide may be required to achieve therapeutic concentrations of inhaled CO in body tissues [Heinemann et al., 2014; Mayr et al., 2005]. Indeed, this drawback impedes the implementation of CO inhalation into clinical praxis. An increase in carboxyhaemoglobin levels beyond 14-15% [Motterlini and Otterbein, 2010] may lead to a shift of the CO-equilibrium, giving rise to tissue accumulation of carbon monoxide. As a consequence, this condition can lead to impairment of cell respiration and thus, cell damage, as previously stated. To avoid this phenomenon, delivery devices for a safe and monitored inhalation of carbon monoxide have been invented recently [Motterlini and Otterbein, 2010]. It remains an open question, whether or not these devices are suitable for this purpose and if parameters can be established to control actual CO levels inside living organisms. Carbon monoxide needs to be delivered in a controllable and ideally tissue-specific manner to prevent adverse drug reactions.

1.4 CO-releasing molecules: Principles of design

The chemical property of carbon monoxide to interact with transition metals has led to the design of molecules that can release CO in a more controllable manner to circumvent the adverse effects of CO inhalation. In fact, these so-called transition metal carbonyls are the basis for the design of the majority of CO-releasing molecules (CORMs). Whereas inhalation of CO has been the leading concept of administration in the early years, CO based therapeutic studies led to a trend towards utilizing CORMs for CO administration. Also, the lack of therapeutic efficacy of CO inhalation on inflammatory parameters in human volunteers [Mayr et al., 2005], and contradictory data in rodent models has discouraged and challenged the route of administration via CO inhalation [Stupfel and Bouley, 1970].
Motterlini *et al.* were the first to discover and identify this novel class of compounds [Motterlini et al., 2002, 2005a]. Ever since, a great variety of CORMs have been designed. This chapter gives a summary of the most important CO-releasing molecules. Generally, the structural design of CORMs can be distinguished into two parts. The core of the compounds has been termed *CORM sphere*, whereas the outer part has been labeled *drug sphere*. The inner part describes the number of CO molecules bound to the metal and its release kinetics. The outer part of the compounds characterizes the pharmaceutical profile [Romao et al., 2012; Schatzschneider, 2015]. There are large variations between the chemical properties, rates of CO release, and release mechanisms of previously proposed CORMs [Motterlini et al., 2005a; Romao et al., 2012; Zobi, 2013]. The mechanisms of release can either be by spontaneous dissociation of carbon monoxide after dissolving in aqueous solutions, or by activation via chemical or physical stimuli [Motterlini R, 2002; Niesel et al., 2008; Pfeiffer et al., 2009; Rimmer et al., 2010; Schatzschneider, 2010, 2011]. The metalcarbonyl complexes CORM-1 and CORM-2 were the first CORMs, and soluble in DMSO. Both the manganese-containing CORM-1 and the ruthenium-containing CORM-2 were shown to have vasoactive properties [Motterlini et al., 2002]. The water-soluble CORM-3 and CORM-A1 liberate carbon monoxide once in contact with physiological solutions [Foresti et al., 2008]. The ruthenium complex CORM-3 shows a rapid CO release, whereas the CORM-A1 possesses a slow rate of CO liberation [Alberto and Motterlini, 2007]. The sodium boranocarbonate CORM-A1 (not being a transition metal complex) shows beneficial effects in terms of vasodilatation [Motterlini et al., 2005b], and cytoprotection [Babu et al., 2015a].

The CO-releasing molecule that has been studied most intensively and is most widely used, is CORM-3. This molecule possesses vasoactive properties [Foresti et al., 2004], antinociceptive effects [Hervera et al., 2013], anti-inflammatory [Bergstraesser et al., 2012; Song et al., 2009] as well as immunomodulatory properties [Masini et al., 2008; Vadori et al., 2009; Yabluchanskiy et al., 2012]. In addition, CORM-3 may provide protection against vascular dysfunction [Mizuguchi et al., 2010; Song et al., 2010] and oxidative damage [Mizuguchi et al., 2010; Motterlini et al., 2012].
In recent years, various photoactivated CO-releasing molecules were designed. In most cases, these so-called photoCORMs contain transition metals and liberate CO when stimulated with UV or visible light [Niesel et al., 2008; Rimmer et al., 2012, 2010]. For these CORMs, topical application might be a promising clinical application route, although further research needs to be performed [Gonzales and Mascharak, 2014; Schatzschneider, 2015]. An interesting property of CORMs in general is, that they do not have a significant impact on the generation of carboxyhaemoglobin; this has been demonstrated by various *in vivo* studies [Motterlini and Otterbein, 2010].
In summary, the different CORMs possess diverse biochemical properties in terms of stability, pharmacokinetic and composition. The outstanding quality of transition metal carbonyls appears to be the possibility to modify the composition or ligands leading to alternation of chemical properties and pharmacokinetic, i.e., the *drug sphere*, as desired [Schatzschneider, 2015]. However, the issue of tissue specificity remains with CO inhalation and the aforementioned CORMs. Additionally, it has to be stated that the latter deliver CO to tissue via passive diffusion. Therefore, it is assumed that higher concentrations are required to achieve effective intracellular levels of carbon monoxide when compared to direct administration of intracellular CO.

1.5 Enzyme-triggered CO-releasing molecules

Enzyme-triggered CO-releasing molecules (ET-CORMs) represent a group of CORMs that use enzymatic cleavage of chemical bonds to release CO. Due to their enzyme specificity, this class of CORMs promise CO delivery with high tissue specificity. The best-studied ET-CORMs are those that are releasing CO intracellularly through the activity of esterase. ET-CORMs are acyloxybutadiene tricarbonyl iron complexes consisting of a mother compound, i.e., 2-cyclohexenone and 1,3-cyclohexanedione, and a type of dienylester ligands at varying positions (Fig. 1.1).
Romanski *et al.* previously showed, that these primarily stable compounds are cleaved only in an esterase dependent manner [Romanski et al., 2012, 2011a, 2013]. Once the compound has entered the cell, intracellular esterases cleave the ester functionality. Subsequent spontaneous oxidative decomposition of the labile enol complex leads to the release of the mother compound, one molecule of ferric iron (Fe^{3+}), and three molecules of carbon monoxide (Fig. 1.2) [Romanski et al., 2012].
ET-CORMs are capable of protecting cells during hypothermic preservation and inhibiting VCAM-1 expression on endothelial and epithelial cells upon TNF-α stimulation. In addition, they induce HO-1 already at low concentrations. At high concentrations and depending on their structure they may have a cytotoxic effect. Likewise, the biological properties of ET-CORMs strongly depend on their chemical structure. Independent of the concentrations, the biological properties of ET-CORMs depend on both the type and position of the ester substituent, as well as the mother compound from which they are derived. ET-CORMs with an ester substituent at the outer

position generally display biological effects (HO-1 induction, VCAM-1 inhibition, toxicity) at lower concentrations compared to ET-CORMs with a substituent at the inner position. The efficacy of ET-CORMs to mediate biological effects decreases with increasing length or complexity of the ester substituent [Romanski et al., 2013; Stamellou, Storz et al., 2014].
Additionally, cell-specific differences in biological activity of ET-CORMs were observed during experiments in RAW267.4 cells, human umbilical vein endothelial cells (HUVEC) and renal proximal tubular epithelial cells (PTEC) [Romanski et al., 2012, 2013]. For instance, the cytotoxic effect of ET-CORMs was more pronounced in HUVEC when compared to PTEC [Romanski et al., 2013]. This effect suggests that PTEC and HUVEC may not have a similar spectrum of esterase enzymes. Depending on the presence of certain esterase enzymes, ET-CORMs may be hydrolysed to release CO intracellularly.

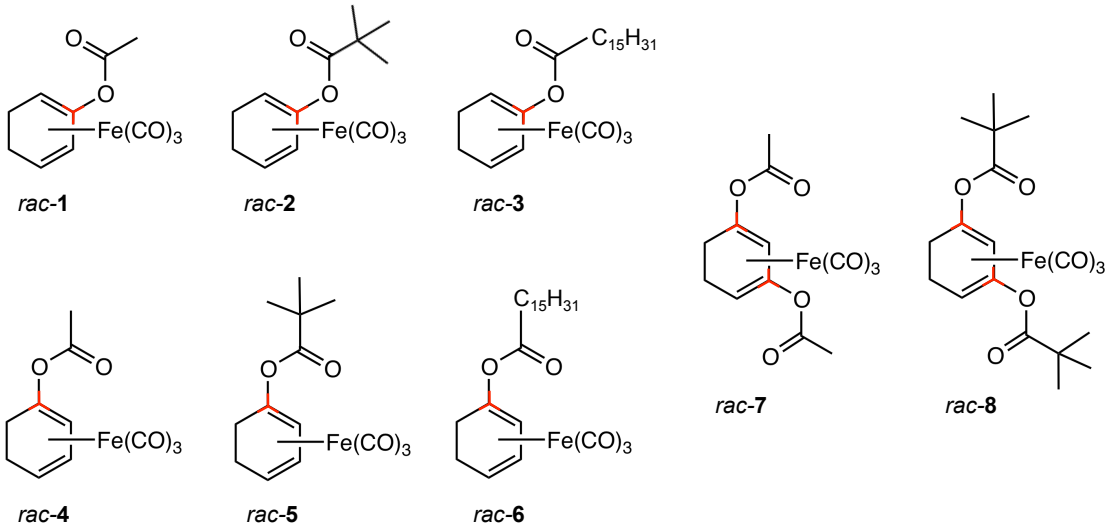

Figure 1.1: Exemplification of ET-CORMs: Exemplification of ET-CORMs showing 2-cyclohexenone derived compounds with the ester functionality at the inner position (top left panel), outer position (bottom left panel) and 1,3-cyclohexanedione derived compounds (panel to the right). Additionally, the various ligands (acetate, pivalate and palmitate) are depicted (own illustration, adapted from Romanski et al. (2013)).

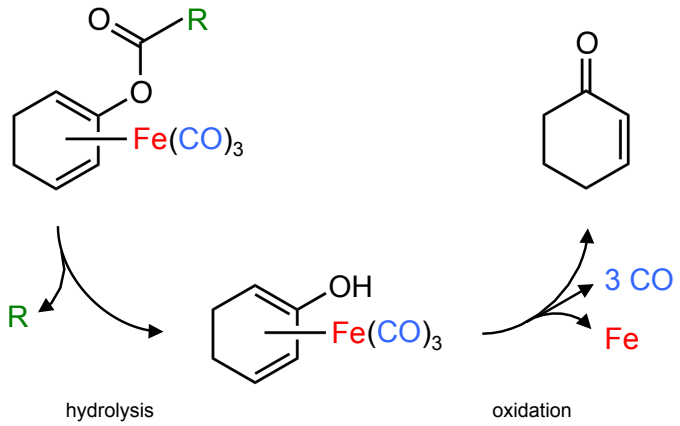

Figure 1.2: Decomposition of ET-CORMs: Decomposition of ET-CORMs (own illustration, adapted from Romanski et al. (2012)).

1.6 Aims of this dissertation

In this work selected ET-CORMs and their properties in terms of cytotoxicity and anti-inflammation in endothelial cells (HUVEC) are investigated to address the question whether this novel class of CORMs may hold advantages over previous forms of CO application. It is examined to what extent variances in cellular uptake or CO release itself are responsible for the characteristic biological activity amongst ET-CORMs and how structural alterations influence these properties. An analysis is conducted to explore whether particularly carbon monoxide mediates the biological effects of these compounds, or whether all by-products of intracellular cleaved ET-CORMs contribute to it. More specifically, the study investigates if cytotoxicity is mediated by release of CO leading to inhibition of cell respiration, or by the concomitant release and potential accumulation of iron. For this analysis, the two 2-cyclohexenone derived ET-CORMs, i.e., *rac*-**1** and *rac*-**4** were selected, as they only differ with respect to the position of the ester functionality. In addition, this work examines the effect of long-term treatment with ET-CORMs on VCAM-1 inhibition. This aspect is studied based on two types of ET-CORMs: The first one being derived from 2-cyclohexenone (*rac*-**1**), the second one being derived from 1,3-cyclohexanedione (*rac*-**8**). Additionally it is studied, if and how these ET-CORMs influence the activation of the transcription factors involved in the regulation of VCAM-1 and HO-1 expression.
Finally, the relevance of structural alterations on biological properties of ET-CORMs was assessed based on enantiomeric compounds. This is motivated by the fact that ET-CORM enantiomers possess the same mother compound and carry the same ester functionality at the same position but differ in the orientation of their functional groups being either in a *trans* or *cis* orientation.

2
Materials and Methods

2.1 | Consumable materials

The following subsection lists consumables, reagents, and analysis kits used in this work.

2.1.1 Chemicals, mediums and reagents

Chemical	*Manufacturer*	*Catalogue number*
Acrylamide mix 40%	Sigma-Aldrich, St. Louis, USA	01708
APS (10%)	Sigma-Aldrich, St. Louis, USA	A3678
Chloroform	Merck Life Science, Darmstadt, Germany	1070242500
Coomassie Protein Assay Reagent	Thermo Fisher Scientific, Waltham, MA, USA	23200
Bovine serum albumin	SERVA, Heidelberg, Germany	11920.06
Deferoxamine	Sigma-Aldrich, St. Louis, USA	D9533-1G
DEPC-treated water	Thermo Fisher Scientific,	AM9915G
DMSO	Sigma-Aldrich, St. Louis, USA	D5879 100 ml
DNase I Amplification Grade	Thermo Fisher Scientific, Waltham, MA, USA	18068015
2,2'-DPD	Sigma, Taufkirchen, Germany	D216305
DTT	Sigma, Taufkirchen, Germany	43819
EDTA solution	Sigma-Aldrich, St. Louis, USA	E7889
Endothelial cell growth medium, 500 ml	Provitro, Berlin, Germany	2011101
Ethanol	Thermo Fisher Scientific, Waltham, MA, USA	9200-1
Ethidium bromide	Sigma, Taufkirchen, Germany	E7637
FCS Gold	PAA, Pasching, Austria	A15-151
Gelatine	Sigma, Taufkirchen, Germany	G7765
Glycine (>99%)	Carl Roth, Karlsruhe, Germany	3908.2
HCl (1 mol/L)	Merck, Darmstadt, Germany	1.09057.1000

HEPES	Sigma, Taufkirchen, Germany	H3375
Hexadimethrine bromide	Sigma, Taufkirchen, Germany	H9268
IMDM Medium, no phenol red	Thermo Fisher Scientific, Waltham, MA, USA	21056-023
Isopropanol	Carl Roth, Karlsruhe, Germany	9866.6
Laemmli Sample Buffer 30 ml	Bio-Rad Laboratories, München, Germany	161-0737
β-mercaptoethanol	Sigma-Aldrich, St. Louis, USA	M7522
Methanol	Carl Roth, Karlsruhe, Germany	HN41.2
Milk powder (blotting grade)	Carl Roth, Karlsruhe, Germany	T145.4
NaCl 0.9% 500 ml	B. Braun, Melsungen, Germany	3570130
NaCl 5 M	Thermo Fisher Scientific, Waltham, MA, USA	24740-011
PageRuler Plus Prestained Protein Ladder	Thermo Fisher Scientific, Waltham, MA, USA	26619
PBS (Dulbecco)	Thermo Fisher Scientific, Waltham, MA, USA	14190-144
PBS (Dulbecco) 10x	Sigma, Taufkirchen, Germany	D1408
Penicillin/Streptomycin	Sigma-Aldrich, St. Louis, USA	P-0781
Phosphatase Inhibitor Cocktail 2 (5 ml)	Sigma-Aldrich, St. Louis, USA	P-5726
Protease Inhibitor Cocktail Tablets, EDTA-free (25 tbl.)	Roche Diagnostics, Mannheim, Germany	11836170001
SDS	Sigma-Aldrich, St. Louis, USA	71725
Sodium deoxycholate	Sigma, Taufkirchen, Germany	D6750
TBS (10x)	Carl Roth, Karlsruhe, Germany	1060.1
TEMED	Sigma-Aldrich, St. Louis, USA	T9281 - 25 ml
Tetrahydrofuran	Merck, Darmstadt, Germany	109731
Thiazolyl Blue Tetrazolium Bromide Reagent (MTT)	Sigma-Aldrich, St. Louis, USA	M2128-5G
TGS buffer for SDS-PAGE (25 mM Tris/ 192 mM Glycine/ 0.1% SDS; pH 8.3) (10x)	Bio-Rad Laboratories	161-0732
TNF-α (recombinant human)	R&D Systems, Wiesbaden, Germany	210-TA
Tris base	Sigma, Taufkirchen, Germany	T1503
Tris-HCl Buffer 0.5 M (pH 6.8)	Bio-Rad Laboratories	161-0799

Tris-HCl Buffer 1.5 M (pH 8.8)	Bio-Rad Laboratories	161-0798
Tris-HCl Buffer 1 M (pH 7.5)	Thermo Fisher Scientific, Waltham, MA, USA	15567-027
Triton X-100	Sigma, Taufkirchen, Germany	X100
TRIzol Reagent	Thermo Fisher Scientific, Waltham, MA, USA	15596-018
Trypsin LE Express	Thermo Fisher Scientific, Waltham, MA, USA	12604-021
TWEEN-20	Sigma-Aldrich, St. Louis, USA	P1379
Western Lightning Plus-ECL, Enhanced Chemiluminescence Subtrate	PerkinElmer Inc., Boston, MA, USA	NEL 103001EA

Table 2.1: Chemicals, mediums and reagents.

2.1.2 Buffers and solutions

Buffer/Solution	*Composition*
Blocking solution for WB	5% milk powder dissolved in PBS
Inactivation solution	5% FCS in PBS
Loading buffer for SDS-PAGE	950 µl of Laemmli sample buffer + 50 µl β-mercaptoethanol
Lysis buffer (ATP)	100 mM Tris, 4 mM EDTA, pH 7.75 in distilled water
Lysis buffer I (protein isolation)	10 mM Tris-HCl, 150 mM NaCl, 5mM EDTA, 1% Triton X-100, 0.5% sodium deoxycholate
Lysis buffer II (protein isolation)	10 mM Tris-HCl, 150 mM NaCl, 5 mM EDTA, 1% Triton X-100, 0.5% sodium deoxycholate + 1 µl DTT, 10 µl phosphatase inhibitor, 150 µl protease inhibitor
Protease Inhibitor	1 tablet of complete EDTA-free Protease Inhibitor was dissolved in 1 ml of PBS
Running buffer for SDS-PAGE (1x)	100 ml of TGS (10x) + 900 ml distilled water
Solubilization solution (MTT)	10% SDS, 0.01 M HCl in distilled water
TBS (1x)	100 ml TBS (10x) + 900 ml distilled water
TBS-Tween 0.1%	1L TBS + 1 ml TWEEN-20
TBS-Tween 0.2%	1L TBS + 2 ml TWEEN-20
Thiazolyl Blue Tetrazolium Bromide Reagent (MTT)	5 mg dissolved in 1 ml distilled water
Transfer buffer for blotting	750 ml distilled water, 150 ml Methanol, 100 ml TGS (10x)

Table 2.2: Prepared buffers and solutions.

2.1.3 Kits

Name	*Manufacturer*	*Catalogue number*
ATP Bioluminescence Assay Kit CLS II	Roche Diagnostics, Mannheim, Germany	11699695001
Cignal Lenti NFκB/Nrf2/positive control Reporter Assay (luc)	Qiagen, Düsseldorf, Germany	CLS-013L, CLS-2020L, CLS-RCL
Cytotoxicity Detection Kit (LDH)	Roche Diagnostics, Mannheim, Germany	11644793001
Dual-Glo Luciferase Assay System	Promega, Mannheim, Germany	E2920
First strand cDNA synthesis Kit	Roche Diagnostics, Mannheim, Germany	11483188001
TaqMan universal PCR master mix, no AmpErase UNG	Thermo Fisher Scientific, Waltham, MA, USA	4324018
TaqMan gene expression assay: hmox1	Thermo Fisher Scientific, Waltham, MA, USA	Hs01110250_m1
TaqMan gene expression assay: GAPDH	Thermo Fisher Scientific, Waltham, MA, USA	Hs02758991_g1

Table 2.3: Kits.

2.2 Devices

Name	*Manufacturer*
ABI PRISM 7700 sequence detection system	Applied biosystems
CASY TT cell counter	Roche Diagnostics
Centrifuge Megafuge	Heraeus Sepatech
Centrifuge Biofuge primo R	Heraeus Sepatech
Centrifuge 5415 C	Eppendorf
DNA Thermal Cycler	Perkin Elmer
Dri-Block heater DB-2D	Techne
Electrophoresis Power Supply EPS 301	General Electric
Fastblot B43, electro-blotting apparatus	Core Life Sciences
Fume hood	Prutscher Laboratory Systems
Fusion SL Vilber Lourmat	Peqlab
Hitachi U-2000 Spectrophotometer	Hitachi, Scientific Istruments
Incubator (5% CO_2, 37°C) Hera cell 150	Heraeus Sepatech
Infinite M200, Microplate Reader	Tecan Group Ltd
Laminar flow hood	Heraeus Sepatech
Magnetic stirrer RCT basic	Ika
Microscope DM IL	Leica
Minigel-Twin for SDS-PAGE	Biometra
Scale Kern 440-33	Kern
Scale Sartorius LP 620 S	Sartorius
Shaker & Mixer Rotamax 120	Heidolph
Shaker & Mixer Polymax 1040	Heidolph
Sonifier W250 (ultrasonic homogenizer)	Branson
Thermal Cycler 2720	Applied biosystems
Vortex-Genie 2	Scientific Industries
Water bath SW-21	Julabo

Table 2.4: Devices and equipment.

2.3 Enzyme-triggered CO-releasing molecules

2.3.1 Acyloxydiene complexes

Acyloxydiene-$Fe(CO)_3$ complexes (ET-CORMs) were synthesized and assessed following the protocols of Romanski *et al.* [Romanski et al., 2012, 2011a, 2013]. The release of CO triggered by esterase was shown for all complexes using headspace gas chromatography (GC) and myoglobin assay. The compounds *rac*-**1** and *rac*-**4** were derived from 2-cyclohexenone (**L1**), whilst *rac*-**8** was derived from 1,3-cyclohexanedione (**L2**). The difference between *rac*-**1** and *rac*-**4** is the position of the ester, being either at the inner (*rac*-**1**) or outer position (*rac*-**4**) of the enone moiety. Both, *rac*-**1** and *rac*-**4**, harbour an acetate moiety while *rac*-**8** has a pivalate as ester substituent at both the inner and outer position. To assess whether the biological activity of ET-CORMs was mediated via release of carbon monoxide or via the organic byproducts after

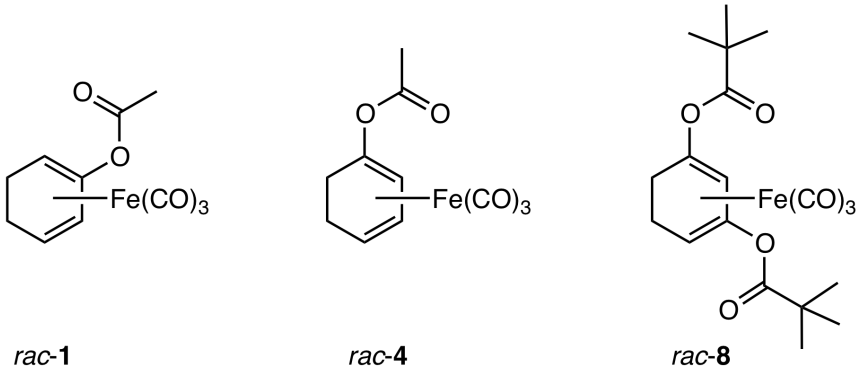

Figure 2.1: ET-CORMs: Chemical structure of the compounds used in the study. The two 2-cyclohexenone derived ET-CORMs, i.e., *rac*-**1** and *rac*-**4**, and the one derived from 1,3-cyclohexanedione (*rac*-**8**) are depicted.

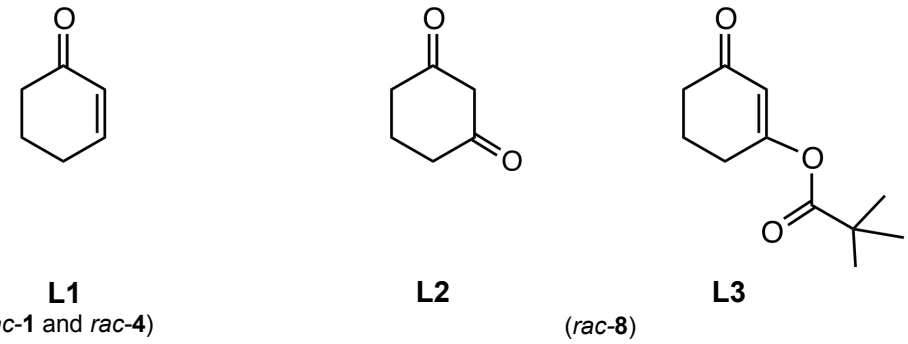

Figure 2.2: Enones: The corresponding hydrolysis products of ET-CORMs resulting from hydrolysis/oxidative desintegration of *rac*-**1** and *rac*-**4** (**L1**) and of *rac*-**8** (**L2** and **L3**) were used to dissect if the hydrolysis products are partly underlying the biological activity of ET-CORMs.

ET-CORM decomposition, the parent compounds of the ET-CORMs used were included in this study. These are 2-cyclohexenone (**L1**), 1,3-cyclohexanedione (**L2**) and composite **L3** formally derived from monohydrolysis and decomplexation of *rac*-**8**. For the experiments, ET-CORMs and their mother compounds were dissolved in DMSO at a concentration of 1 mM and stored at -20°C until usage. The chemical structures and annotations of the compounds are shown in Figs. 2.1 and 2.2.

2.3.2 Cyclodextrin encapsulated ET-CORMs

The compounds *rac*-**1** and *rac*-**4** were additionally used as randomly methylated-beta-cyclodextrin (RAMEB) complexes in cell culture experiments, to assess if the difference in their bioactivity was due to a differential cellular uptake of these ET-CORMs. For this purpose, 2.4 mg (8.75 µmol) of *rac*-**1** or 2.8 mg (10 µmol) *rac*-**4** were added to a water solution of 41.25 mM (or 40 mM, respectively) of RAMEB. The chemical formation of the complexes was achieved by treating the samples in an ultrasonic bath for 30 minutes at 80°C. To assess release of carbon monoxide

from ET-CORM/RAMEB complexes CO Probe 1 (COP-1) was used. For this purpose, COP-1 (10 μM), the ET-CORM/RAMEB complexes (RAMEB@*rac*-**1** and RAMEB@*rac*-**4**) (each 100 μM) and pig liver esterase (3 U/ml) were incubated in 96-well plates for various time points. Pig liver esterase was substituted for HUVEC cell lysates (10 μg/ml) as an esterase source in some experiments. The cell lysates were prepared by repeated cycles of freeze-thawing in PBS. In all experiments controls were included by omitting pig liver esterase or cell lysate. The fluorescence intensity was measured at an excitation wavelength of 475 nm and an emission wavelength of 510 nm. Fluorescence intensity of the controls was subtracted for each condition.

2.3.3 ET-CORMs as enantiomers

To evaluate the biological activity in relation to the structure of the compound in a more detailed manner, and to furthermore optimize the chemical substance, enantiomers of ET-CORMs were synthesized [Romanski, 2013]. The geometric isomers of ET-CORMs used in this thesis are divided accordingly into two groups. The first group comprises trans-enantiomers, i.e., Stro 786-**A** and Stro 790-**A**, and the second group consists of cis-enantiomers, i.e., Stro 786-**C** and Stro 790-**C**. However, there are also structural differences within one group. Compound Stro 786-**C** harbours the substituent groups facing upwards, whereas substituent groups of Stro 790-**C** facing downwards when comparing with the plane. For experiments, ET-CORM enantiomers were dissolved in DMSO at a concentration of 1 mM and stored at -20°C until usage.

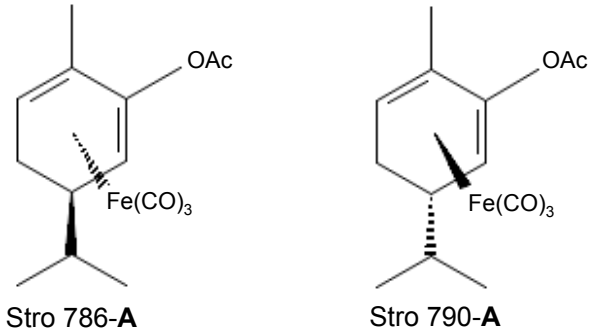

Figure 2.3: Trans-enantiomers.

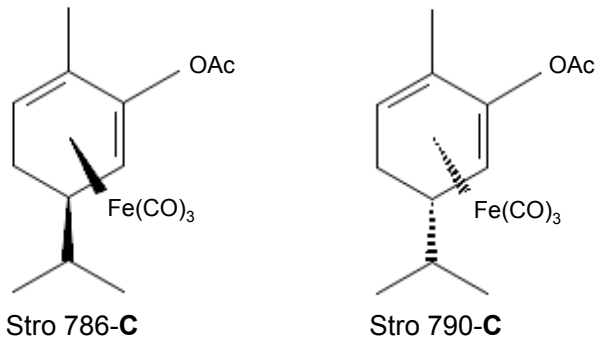

Figure 2.4: Cis-enantiomers.

2.4 Experimental Methods

2.4.1 Cell culture

Human umbilical vein endothelial cells (HUVEC) were purchased from Promo Cell, Heidelberg, Germany. HUVEC were cultured in basal endothelial medium supplemented with 10% FCS, essential growth factors and antibiotics (Penicillin/Streptomycin) in T75 flasks in a 5% CO_2-humidified atmosphere at 37°C until confluence.
For cell passaging, cells were washed with PBS and trypsinized for 5 minutes at 37°C. Inactivation solution (5% FCS in PBS) was added and cells were harvested. Flasks were washed with PBS to collect remaining cells. Cell detachment of HUVEC from the flask was monitored using a microscope. Cell suspension was centrifuged for 5 minutes at 1200 rpm at room temperature. After aspirating supernatant, cell pellet was resuspended in appropriate HUVEC medium and seeded into appropriate flasks or wells (passaging in a relation of 1:3). Flasks and wells were prepared for seeding with filtered 1% gelatine for 15-30 minutes at RT. Experiments with HUVEC were conducted on cells in passages 4-6 at approximately 80-90% confluence.

2.4.2 Evaluation of intracellular proteins

Protein isolation

After cells were stimulated with TNF-α (10 ng/ml) and different concentrations of ET-CORMs depending on the experiment, proteins were isolated for further investigations. Prepared Inactivation solution, PBS and Trypsin were stored in water bath at 37°C. Cell extracts were made from trypsinized HUVEC by resuspending the cell pellet in 50 µl of lysis buffer II (10 mM Tris-HCl, 150 mM NaCl, 5 mM EDTA, 1% triton X-100 and 0.5% sodium deoxycholate, 1 µl of freshly prepared DTT, 150 µl protease inhibitor and 10 µl phosphatase inhibitor). The lysate was transferred into 1.5 ml Eppendorf tubes and incubated for 5 minutes on ice. Hereafter the samples were centrifuged at 14000 rpm for 10 minutes at 4°C. Supernatants were transferred into new 1.5 ml Eppendorf tubes and stored at -20°C until use.

Protein quantification

Total protein concentration of extracts was measured according to Bradford [Bradford, 1976]. Samples were diluted to 1:10 with NaCl 0.9% and 1 ml of Coomassie-Reagent was added to each Eppendorf tube. After 10 minutes of incubation at RT optical density at 595 nm (OD595) of the samples were measured by a spectrophotometer (Hitachi U-2000). Protein concentrations were calculated based on a standard curve of known protein concentrations.

SDS-PAGE and Western blotting

For the polyacrylamide gel electrophoresis 10% SDS-gels were prepared. The running gel was mixed according to Tab. 2.5 and immediately poured to assembled gel casting unit, leaving 2-3 cm space for the stacking gel. 500 µl of isopropanol was added to the casting unit to ensure a straight boundary between running and stacking gel. After polymerisation isopropanol was removed, the stacking gel prepared and poured on top of running gel. A comb with ten cavities (capacity each 15-18 µl) was inserted in the stacking gel. After polymerisation of the gel, the

	Stacking gel	*Running gel*
dH2O	3.6 ml	4.8 ml
Acrylamide mix 40%	620 µl	2.5 ml
Tris-HCl 1.5 M (pH 8.8)	-	2.5 ml
Tris-HCl 0.5 M (pH 6.8)	630 µl	-
SDS 10%	50 µl	100 µl
TEMED	5 µl	4 µl
APS 10%	50 µl	100 µl

Table 2.5: Composition of SDS-gel.

Antibody	*Manufacturer*	*Catalogue number*
Anti-β-actin (monoclonal, mouse)	Sigma, Taufkirchen, Germany	A5441
Anti-GAPDH (monoclonal, mouse)	Abcam, Cambridge, USA	ab9484
Anti-HO-1 (polyclonal, rabbit)	Enzo, Lörrach, Germany	ADI-SPA-896
Anti-IκBα (polyclonal, rabbit)	Santa Cruz Biotechnology, Heidelberg, Germany	sc-371
Anti-VCAM-1 (polyclonal, rabbit)	Cell Signaling Technology, Boston, USA	12367S
Secondary antibodies (conjugated with horseradish peroxidase)	Santa Cruz Biotechnology, Heidelberg, Germany	
- goat anti-rabbit IgG-HRP		sc-2004
- goat anti-mouse IgG-HRP		sc-2005

Table 2.6: Antibodies for Western blotting.

casting unit was transferred to the electrophoresis chamber. Subsequently, the chamber was filled with running buffer.
20 µg of protein extract (or otherwise specified) was mixed with loading buffer in the ratio 1:1. Subsequently the samples were incubated for 5 minutes at 100°C, followed by short centrifugation and incubation for 5 minutes on ice. Electrophoresis was initiated using 80 mV for 20-30 minutes for stacking of the samples, hereafter the gels were run at 130 mV for approximately 90 minutes. After electrophoresis, proteins were transferred by semi-dry blotting to a PVDF western blotting membrane (Roche Diagnostics) according to standard operating procedures. The membranes were blocked in blocking buffer for 1 hour at RT on a shaker to prevent unspecific background staining. Hereafter, blots were incubated overnight at 4°C with polyclonal anti-VCAM-1 (dilution 1:1000), polyclonal anti-IκBα (dilution 1:1000), polyclonal anti-HO-1 (dilution 1:1000), monoclonal anti-β-actin antibody (dilution 1:5000) or anti-GAPDH antibody (dilution 1:5000) (all dilutions in blocking buffer). The membranes were thoroughly washed in TBS-Tween 0.1% and then incubated for 1 hour at room temperature with the appropriate IgG-Horseradish peroxidase secondary antibody in blocking buffer (dilution 1:2000, Tab. 2.6). Subsequently, the membranes were washed in

TBS-Tween 0.1% 5 times for 5 minutes each. Protein bands were visualized by using enhanced chemiluminescence substrate following the manufacturer's instructions (PerkinElmer Inc., USA).

2.4.3 Cell toxicity

MTT Cell toxicity assay

HUVEC were cultured in 96-well plates until confluence. Subsequently, cells were treated with different concentrations of *rac*-**1**, *rac*-**4** either dissolved in DMSO or as RAMEB complexes, as well as with ET-CORM enantiomers for the indicated time periods. In some experiments, HUVEC were treated for 24 hours with serial dilutions of $FeCl_2$ or $FeCl_3$ or *rac*-**4** (100 μM) in the presence or absence of iron chelators deferoxamine (80 μM) or 2,2-DPD (100 μM). Deferoxamine was added to the cells at the time of stimulation with ET-CORMs, whereas 100 μM 2,2'-DPD was used for 1 hour prior to stimulation. Assessment of cytotoxicity was performed using the 3-(4,5-dimethylthiazol-2-yl)-2,5-diphenyl tetrazolium bromide (MTT) assay. At the indicated times, 10 μl of 5 mg/ml MTT reagent was added to each well generating a light yellow solution, following incubation for 4 hours at 37°C and in 5% CO_2 atmosphere. Hereafter 100 μl of solubilisation solution was added to each well to dissolve the purple formazan crystals and the plates were incubated overnight at 37°C, 5% CO_2. Absorbance was measured the next day at a wavelength of 550 nm with a reference wavelength 690 nm using Infinite M200 Microplate reader. Cell viability was expressed as percentage of viable cells relative to the untreated cells. All experimental conditions were tested in triplicates in at least 4 different experiments.

LDH Cytotoxicity assay

To assess the effects of ET-CORM enantiomers during cold preservation injury, the cytotoxicity detection kit (LDH, Roche Diagnostics) was used. To this end, HUVEC were cultured in 24-well plates until confluence. While adding ET-CORM enantiomers for stimulation, the medium was changed to IMDM phenol free medium (without supplements) to avoid interactions of phenol red with the LDH cytotoxicity kit. Subsequently, cells were placed on ice at 4°C for 24 hours. LDH was measured according to the manufacturer's instructions. Absorbance was measured at 490 nm with 620 nm as reference wavelength. All experiments were tested in triplicates in 3 independent experiments.

2.4.4 Intracellular ATP Measurement

Intracellular ATP concentration was assessed by performing a bioluminescence assay (Roche Diagnostics). HUVEC were cultured in 24-well plates until confluence. Subsequently, cells were treated with different concentrations of *rac*-**1** and *rac*-**4** for a certain period of time (15 min, 60 min or 24 h depending on the specific experiment). Cells were washed twice in PBS. 200 μl of lysis buffer (ATP) was added to each well and the 24-well plate was incubated for 10 minutes at RT on a shaker. Cell lysates containing intracellular ATP were harvested and distributed to cavities of a 96-well plate, 50 μl of samples per cavity. Subsequently, 50 μl of luciferase from freshly prepared luciferase reagent (10 ml of ddH_2O added to luciferase reagent, 5 minutes incubation at 4°C) was added to each well followed by immediate measurement of luminescence. An ATP Standard was serial diluted from 16.5 mM $\times 10^{-5}$ until 16.5 mM $\times 10^{-11}$ and included in each experiment. All experimental conditions were tested in triplicates in at least 3 different experiments.

2.4.5 Detection of intracellular CO-release

CO Probe 1 (COP-1), a reaction-based fluorescent substrate, was used to assess intracellular release of CO and was synthesized as reported [Michel et al., 2012]. To catalyze ET-CORMs, pig liver esterase (3 U/ml) or HUVEC cell lysates (10 µg/ml; prepared by freeze-thawing in PBS) were incubated with 1 µl/ml (final concentration 10 µM) of COP-1 in the presence of ET-CORMs (100 µM) in a 96-well plate at 37°C for various time points. Controls were included by omitting pig liver esterase or cell lysate. The fluorescence, based on Palladium-mediated carbonylation, was measured at an emission wavelength of 510 nm and excitation wavelength of 475 nm. For each condition the fluorescence intensity of the controls was subtracted. In addition to fluorescence measurement, confocal microscopy was used to visualize CO-release with COP-1.

2.4.6 Reporter assay

HUVEC were cultured in 96-well plates and transduced with commercially available lentiviral particles containing an inducible NFκB or Nrf2 luciferase reporter (Qiagen, Germany). The medium was removed from the cavities and 20 µl of Cignal lenti particles were added. Subsequently, cell growth medium was added to each well, following incubation at 37°C in an atmosphere of 5% CO_2. For each condition, transduction efficiency was assessed with a constitutively expressed luciferase construct. Two days after transduction, the medium was removed and cells were stimulated with TNF-α (10 ng/ml) and/or different concentrations of ET-CORMs in triplicates for 24 hours. Luciferase activity measurements were performed following the manufacturer's protocol (Promega, Germany). Dual-Glo Luciferase Reagent and Dual-Glo Stop & Glo Reagent were prepared. 50 µl Dual-Glo Luciferase Reagent was added to each well, followed by incubation of 10 minutes at RT. Firefly luminescence was measured. Subsequently, 50 µl Dual-Glo Stop & Glo Reagent was added following incubation of 10 minutes at RT and measurement of renilla luminescence. Inducible luciferase expression was normalized for constitutively expressed luciferase to control differences in transduction efficiency. The data of 4 independent experiments are expressed as mean fold increase ± standard deviation relative to the control.

2.4.7 Isolation of RNA and qPCR

To isolate total RNA from cultured HUVEC, cells were trypsinized and washed after 24 hours of stimulation with *rac*-**1** or *rac*-**8**. Each cell pellet was subsequently resolved with TRIzol Reagent 1 ml per 10^7 cells and incubated for 10 minutes at RT for complete dissociation of nucleoprotein complexes. Hereafter 200 µl of Chloroform was added, shaken and incubated for 3 minutes at RT. Samples were centrifuged at 12000 rcf and 4°C for 15 minutes. The aqueous phase containing total RNA, was transferred to fresh, RNase-free Eppendorf tubes and 0.5 ml of isopropanol was added to precipitate the RNA. After centrifugation at 12000 rcf and 4°C for 10 minutes, pellets were washed twice with 1 ml ethanol 75%. After the final centrifugation at 7500 rcf for 5 minutes, the RNA pellets were air dried and dissolved in 20 µl of DEPC-treated water. RNA concentration was measured with the Infinite M200 Microplate Reader and samples were stored at -80°C until further use.
To eliminate DNA from the samples, DNase treatment was performed prior to qPCR using the DNase I Amplification Grade (Thermo Fisher Scientific). Samples were thawed at RT. DNase I Reaction Buffer at a concentration of 10% of the sample volume and 1 µl of DNase I Amp Grade (1 U/µl) were added. Subsequently, the solution was filled up to 10 µl with DEPC-treated water followed by incubation for 15 minutes at RT. 1 µl of EDTA (25 mM) was added to inactivate

the DNase and to avoid Mg^{2+}-dependent hydrolysis of RNA. Eppendorf tubes were heated for 10 minutes at 65°C and were immediately put on ice afterwards.
1 µg of total RNA was reverse transcribed into cDNA using the first strand cDNA synthesis kit (Roche Diagnostics, Tab. 2.7). Components were mixed gently, following reverse transcriptase reaction using Thermal Cycler 2720 (Applied biosystems) with the following setting:

- 10 minutes at 25°C
- 60 minutes at 42°C
- 5 minutes at 99°C
- 5 minutes at 4°C

cDNA was diluted in 20 µl DEPC-treated water and stored at -20°C until usage. Samples were evaluated in 1% agarose gel electrophoresis with supplement of ethidium bromide.

Component	*Volume (total 20 µl)*
RNA sample (DNase treated)	1 µg
10x Reaction Buffer	2 µl
25 mM $MgCl_2$	4 µl
Deoxynucleotide Mix	2 µl
Oligo-p$(dT)_{15}$ Primer	2 µl
RNase Inhibitor	1 µl
AMV Reverse Transcriptase	0.8 µl

Table 2.7: First strand cDNA synthesis.

Real-time quantitative PCR was performed on an ABI PRISM 7700 sequence detection system (Applied biosystems) using TaqMan universal PCR master mix, no AmpErase UNG. For the quantification of gene expression of interest, TaqMan gene expression assays for HO-1 (hmox1) and GAPDH were used (all Thermo Fisher Scientific, Tab. 2.3). Reaction mix was prepared accordingly and samples were run under the following conditions:

1) Initial denaturation for 10 minutes at 95°C, followed by
2) 40 cycles of
    - denaturation for 15 seconds at 95°C and
    - annealing/extension for 1 minute at 60°C.

The comparative cycle threshold method ($\Delta\Delta C_T$ method) was used to determine the levels of gene expression in each sample. The levels of the target gene (hmox1) were referred to the levels of the reference gene (GAPDH), whose expression is not influenced. The efficiency of the PCR was assessed from the slopes of the standard curves and was found to be between 90% and 100%. Linearity of the assay could be demonstrated by serial dilution of all standards and cDNA. All samples were normalized for an equal expression of GAPDH.
Equation of the $\Delta\Delta C_T$ method:

$$\Delta\Delta C_T = \Delta C_{T(\text{treated})} - \Delta C_{T(\text{control})}$$
$$\Delta\Delta C_T = \left[(Ct_{\text{target gene}} - Ct_{\text{target gene}})_{\text{treated}} - (Ct_{\text{target gene}} - Ct_{\text{target gene}})_{\text{control}}\right]$$
$$2^{-\Delta\Delta C_T} = \text{fold change due to treatment}$$

2.5 Statistical analysis

All data are expressed as the mean ± standard deviation unless otherwise specified. At least three independent experiments were performed. Statistical significance was assessed by One-way-ANOVA and student's *t*-test. P-value of $P < 0.05$ was considered as significant. GraphPad Prism (GraphPad Software, Inc., La Jolla, USA) was used for calculation of EC_{50} values and curve fitting. Statistical analysis for the data of ET-CORMs was performed by Eleni Stamellou.

3
Results

3.1 | ET-CORMs as enantiomers

Enantiomers describe the three-dimensional position of their substituent group. Stro 786-**A** and Stro 790-**A** represent trans-enantiomers with the substituent group facing upwards (Stro 786-**A**) or downwards (Stro 790-**A**), while Stro 786-**C** and Stro 790-**C** are the cis-enantiomers of the same structure (Figs. 2.3 and 2.4). This study assessed if the two enantiomers of ET-CORMs behave different with respect to the biological activity that was tested (toxicity, inhibition of VCAM-1, induction of HO-1 and protection against cold inflicted injury of endothelial cells).

3.1.1 Cytotoxicity, VCAM-1 inhibition and HO-1 induction

Cytotoxicity in HUVEC cell cultures, measured after 24 hours of stimulation with the test compounds, was consistently more pronounced for the cis-compounds, i.e., Stro 786-**C** and Stro 790-**C**, when compared to the trans-compounds (Stro 786-**A** and Stro 790-**A**) at concentrations of 25 μM up to 100 μM (Fig. 3.1). Within the cis-compounds itself, Stro 790-**C** was more toxic than Stro 786-**C**. These differences were not found for the trans-enantiomers Stro 786-**A** and Stro 790-**A**. ET-CORM enantiomers can effectively inhibit TNF-α mediated VCAM-1 expression as demonstrated by Western blotting (Fig. 3.2). Whereas the trans-enantiomers inhibit VCAM-1 expression at a concentration of 50 μM, for the cis-enantiomers a strong inhibition was noted already at 25 μM. Hence, similar as mentioned for cytotoxicity, the cis-enantiomers seem to be more effective than the trans-enantiomers, and within the cis-enantiomers, Stro 790-**C** inhibits VCAM-1 much stronger than Stro 786-**C** when compared at a concentration of 25 μM. Interestingly, Stro 790-**C** seems to inhibit VCAM-1 more effectively at a concentration of 25 μM in comparison to 50 μM of Stro 786-**A** and Stro 790-**A**. In addition to VCAM-1 inhibition, this study assessed the ability of the enantiomers to induce HO-1 expression. Comparable to VCAM-1 inhibition, cis-enantiomers (25 μM) induce HO-1 more effectively when compared to trans-enantiomers (50 μM or 25 μM).

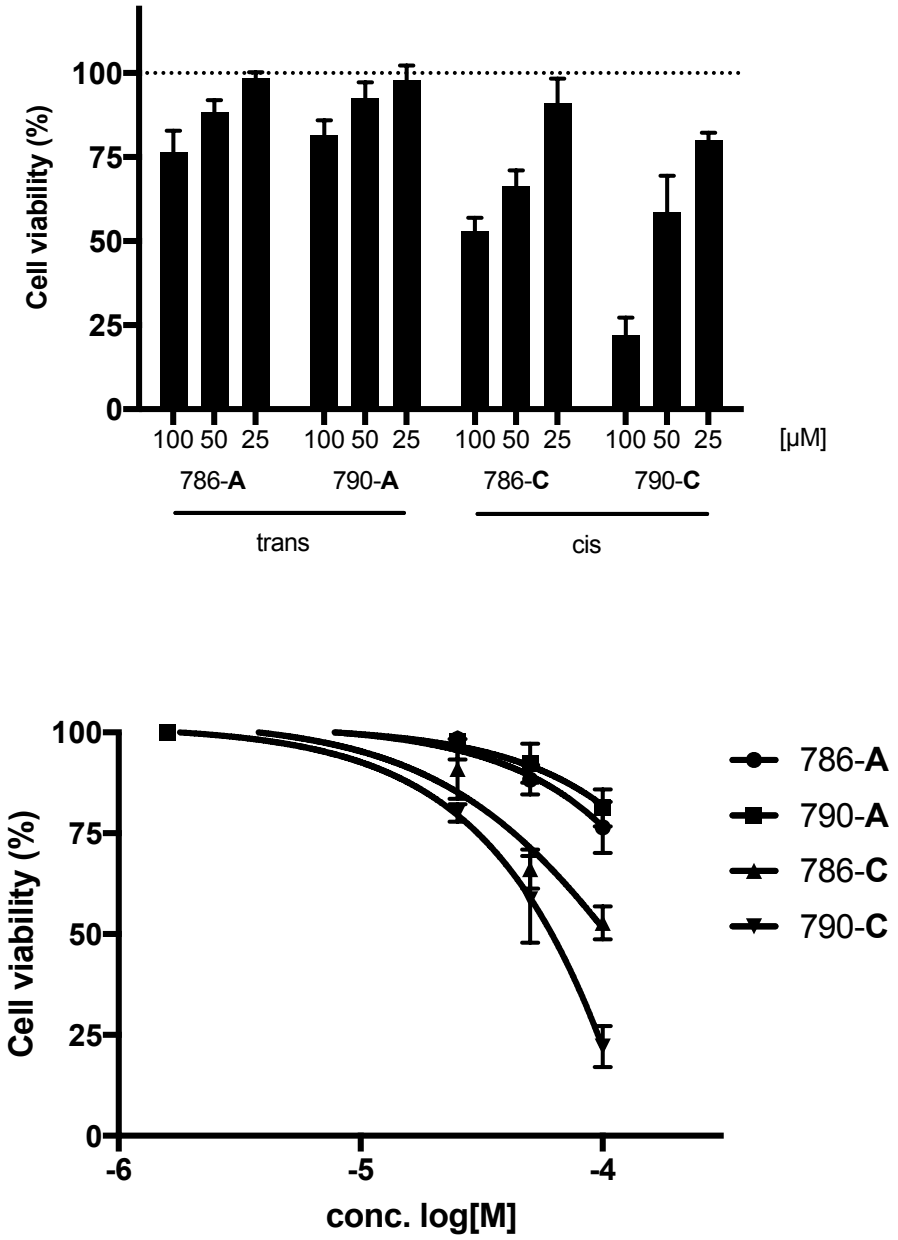

Figure 3.1: Cytotoxicity of ET-CORM enantiomers: HUVEC were grown in a 96-well plate until confluence and subsequently treated for 24 hours with different concentrations of ET-CORM enantiomers. MTT cytotoxicity assays were performed as mentioned in the methods section. The data of a representative experiment are depicted. The results are expressed as mean % of cell viability ± SD, relative to the untreated HUVEC. All conditions were tested in triplicates in 3 different experiments.

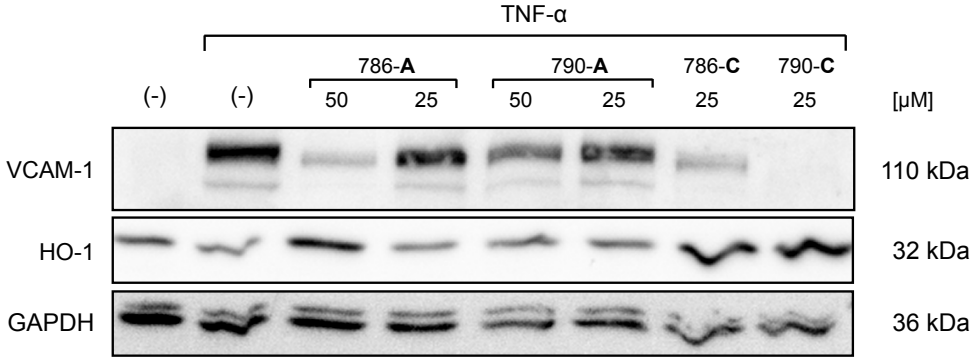

Figure 3.2: Inhibition of VCAM-1 and induction of HO-1 by ET-CORM enantiomers: HUVEC were grown in 24-well plates until confluence. To demonstrate whether ET-CORM enantiomers have an influence on VCAM-1 and HO-1 expression, cells were stimulated with TNF-α for 24 hours in the presence or absence of different concentrations of ET-CORM enantiomers. VCAM-1 and HO-1 expression was assessed by Western blotting, GAPDH was used as loading control. Data of a representative experiment are shown. At least 4 independent experiments have been performed with essentially the same result.

3.1.2 Cold preservation injury

As demonstrated by light microscopy and LDH release, ET-CORM enantiomers displayed protection against cell damage occurring after 24 hours of cold preservation (at 4°C) of HUVEC (Figs. 3.3 and 3.4). At a concentration of 25 μM, the cis-enantiomers showed comparable protective effects, which were more pronounced compared to the trans-enantiomers. Cell damage and cell integrity evaluated by light microscopy prior to LDH detection clearly displayed a higher tolerance to hypother-mia when HUVEC were treated with ET-CORM enantiomers (Fig. 3.4).

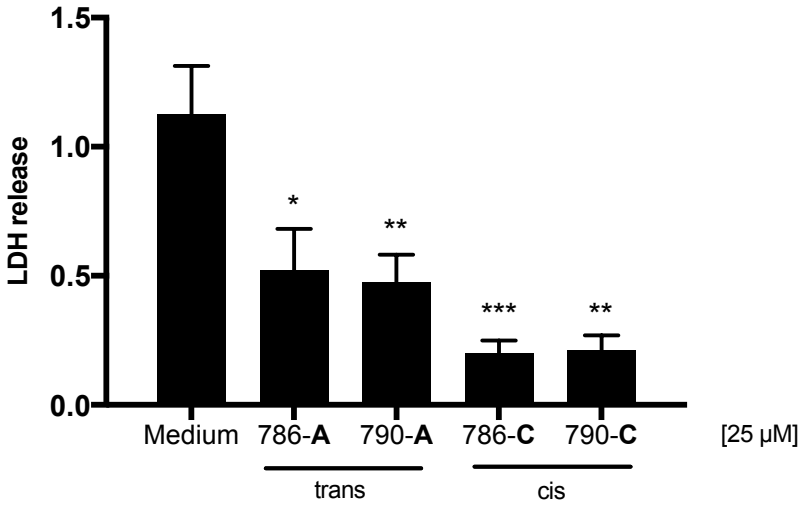

Figure 3.3: LDH release during cold preservation by ET-CORM enantiomers: HUVEC were cultured in a 24-well plate until confluence. Cells were stimulated with 25 μM of different ET-CORM enantiomers in IMDM phenol free medium. Subsequently, cells were put on ice and stored at 4°C for 24 hours. Supernatant was harvested and LDH cytotoxicity detection kit (Roche Diagnostics) was used to assess the tolerance to hypothermia-associated cell damage as described in the methods section. Untreated cells (medium) served as control. The data expressed as mean LDH release ± SD of a representative experiment are depicted, $* P < 0.05$, $** P < 0.01$, $*** P < 0.001$. All conditions were tested in triplicates in 3 independent experiments.

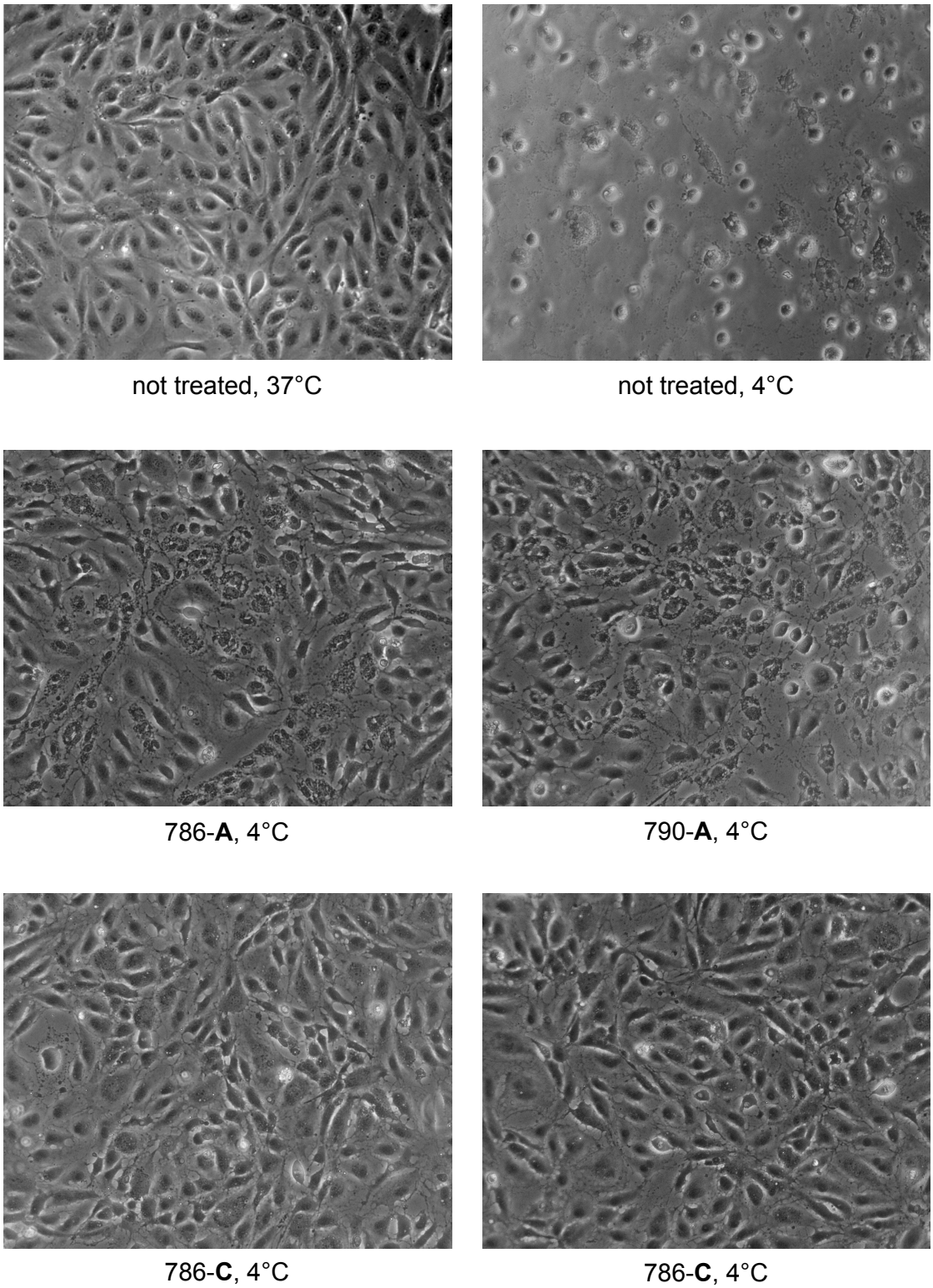

Figure 3.4: Tolerance to hypothermia due to treatment with ET-CORM enantiomers: Microscope images showing HUVEC after 24 hours of cold preservation. HUVEC were microscopically evaluated after 24 hours of cold preservation at 4°C in the presence or absence of ET-CORM enantiomers [25 µM]. HUVEC not treated with ET-CORM enantiomers and cultured at 37°C served as control. Original magnification: 10x.

3.2 | ET-CORMs

The following results have been published in Redox Biology (2014) 2:739-748 "Different design of enzyme-triggered CO-releasing molecules (ET-CORMs) reveals quantitative differences in biological activities in terms of toxicity and inflammation." by Stamellou E. and Storz D. as equally contributing first authors. My contribution to this publication was the performance of experiments, acquisition of data, illustration of figures, and drafting of the paper. The content of this part is depicted in extended form.

3.2.1 CO release, toxicity and intracellular ATP concentrations

Although the 2-cyclohexenone derived ET-CORMs *rac*-**1** and *rac*-**4** (Fig. 2.1) display minor structural differences, i.e., the position of the ester functionality, they strongly differ with respect to cytotoxicity [Romanski et al., 2013]. Because cellular uptake of cyclodextrin-formulated compounds predominantly depends on structural entities of the cyclodextrin polymer rather than that of the compounds it encapsulates, *rac*-**1** and *rac*-**4** were prepared as such RAMEB@*rac*-**1** and RAMEB@*rac*-**4** respectively, to assess whether the differences in cytotoxicity were caused by quantitative differences in cellular uptake or by spatiotemporal differences in CO release. CO was still released from the cyclodextrin-formulated compounds, as demonstrated by a time-dependent increase in fluorescence intensity when COP-1 was incubated with RAMEB@*rac*-**1** and RAMEB@*rac*-**4** in the presence of pig liver esterase or lysates of HUVEC as esterase source (Fig. 3.5). CO release in this assay was significantly higher for RAMEB@*rac*-**4** as compared to RAMEB@*rac*-**1** and was more pronounced when lysates from HUVEC were used. When HUVEC were cultured for 24 hours with different concentrations of *rac*-**1** and *rac*-**4,** either dissolved in DMSO or used as cyclodextrin formulation, rac-**4** was consistently more toxic compared to *rac*-**1** irrespective of the formulation (EC_{50} [μM] *rac*-**1** vs. *rac*-**4**: 448.9 ± 50.23 vs. 8.2 ± 1.5, EC_{50} [μM] RAMEB@*rac*-**1** vs. RAMEB@*rac*-**4**: 457.3 ± 8.23 vs. 7.22 ± 1.12) (Fig. 3.6). Based on the notion that cellular uptake of the cyclodextrin-formulated RAMEB@*rac*-**4** and RAMEB@*rac*-**1** is equal, the present data indicate that RAMEB@*rac*-**4** is significantly more toxic as a consequence of a higher CO release as compared to RAMEB@*rac*-**1**.
Cell toxicity was also observed when HUVEC were incubated with $FeCl_2$ or $FeCl_3$ (Fig. 3.7, top graph), indicating a potential deleterious role for the concomitantly released iron upon ET-CORM hydrolysis. However, EC_{50} values for *rac*-**4** were significantly lower compared to $FeCl_2$ or $FeCl_3$ (EC_{50} $FeCl_3$ vs. *rac*-**4**, ∼ 120 vs. 8.2 ± 1.5 [μM]) and were neither influenced by deferoxamine (Fig. 3.7, bottom graph) nor by the more cell membrane permeable 2,2'-dipyridyl (2,2-DPD) iron chelator (data not shown). Interestingly, intracellular ATP concentrations were slightly increased at low concentrations of both *rac*-**1** and *rac*-**4**, while at high concentrations intracellular ATP strongly diminished in HUVEC that were treated with *rac*-**4** but not with *rac*-**1** (Fig. 3.8, top graph). When 100 μM of *rac*-**4** was added to HUVEC, ATP concentrations already diminished within 15 minutes (Fig. 3.8, bottom graph).

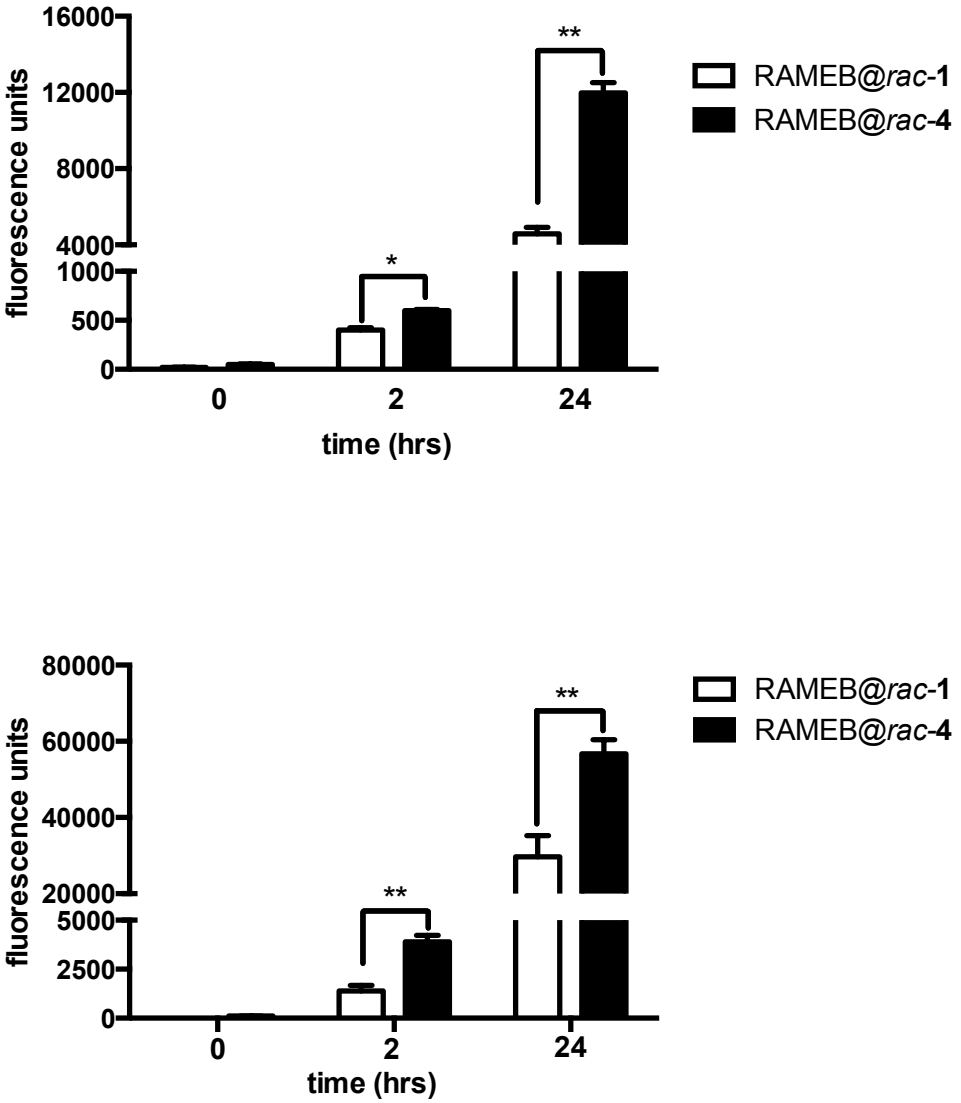

Figure 3.5: Release of CO by cyclodextrin formulated ET-CORMs: CO release from *rac*-**1** and *rac*-**4** in cyclodextrin formulation RAMEB@*rac*-**1** and RAMEB@*rac*-**4** respectively was assessed by measuring COP-1 fluorescence intensity. To this end, COP-1 (10 μM), RAMEB@*rac*-**1** and RAMEB@*rac*-**4** (100 μM for both) and pig liver esterase (3 U/ml) (top graph) or cell lysates from HUVEC (10 μg/ml) (bottom graph) were incubated in 96-well plates for various time points. In all experiments controls were included by omitting pig liver esterase or cell lysate. Fluorescence intensity of the controls was subtracted from the fluorescence intensity of each condition. The results of 3 independent experiments are depicted as mean fluorescence intensity in arbitrary units ± SD, $*$ $P < 0.05$, $**$ $P < 0.01$.

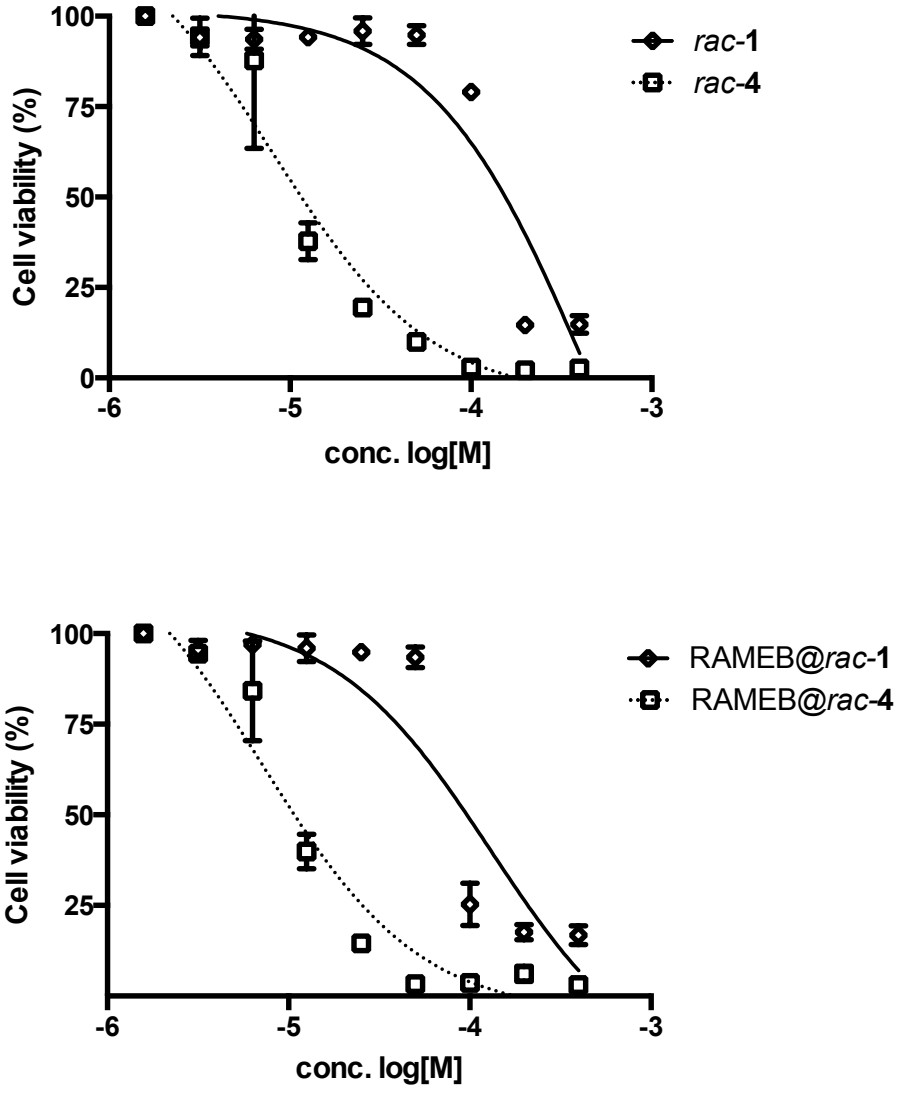

Figure 3.6: Cytotoxicity for *rac*-**1**, *rac*-**4** and cyclodextrin encapsulated ET-CORMs: HUVEC were grown in 96-well plates until confluence and subsequently stimulated for 24 hours with different concentrations (0 µM to 200 µM) of *rac*-**1**, or *rac*-**4** either dissolved in DMSO (top graph) or as cyclodextrin formulation RAMEB@*rac*-**1** and RAMEB@*rac*-**4** (bottom graph). Toxicity was assessed by MTT assay, each concentration was tested in triplicate in all experiments. The results of 3 independent experiments are expressed as mean % of cell viability ± SD, relative to the untreated HUVEC. The corresponding EC_{50} [µM] were: *rac*-**1** vs. *rac*-**4**: 448.9 ± 50.23 vs. 8.2 ± 1.5, EC_{50} [µM] RAMEB@*rac*-**1** vs. RAMEB@*rac*-**4**: 457.3 ± 8.23 vs. 7.22 ± 1.12.

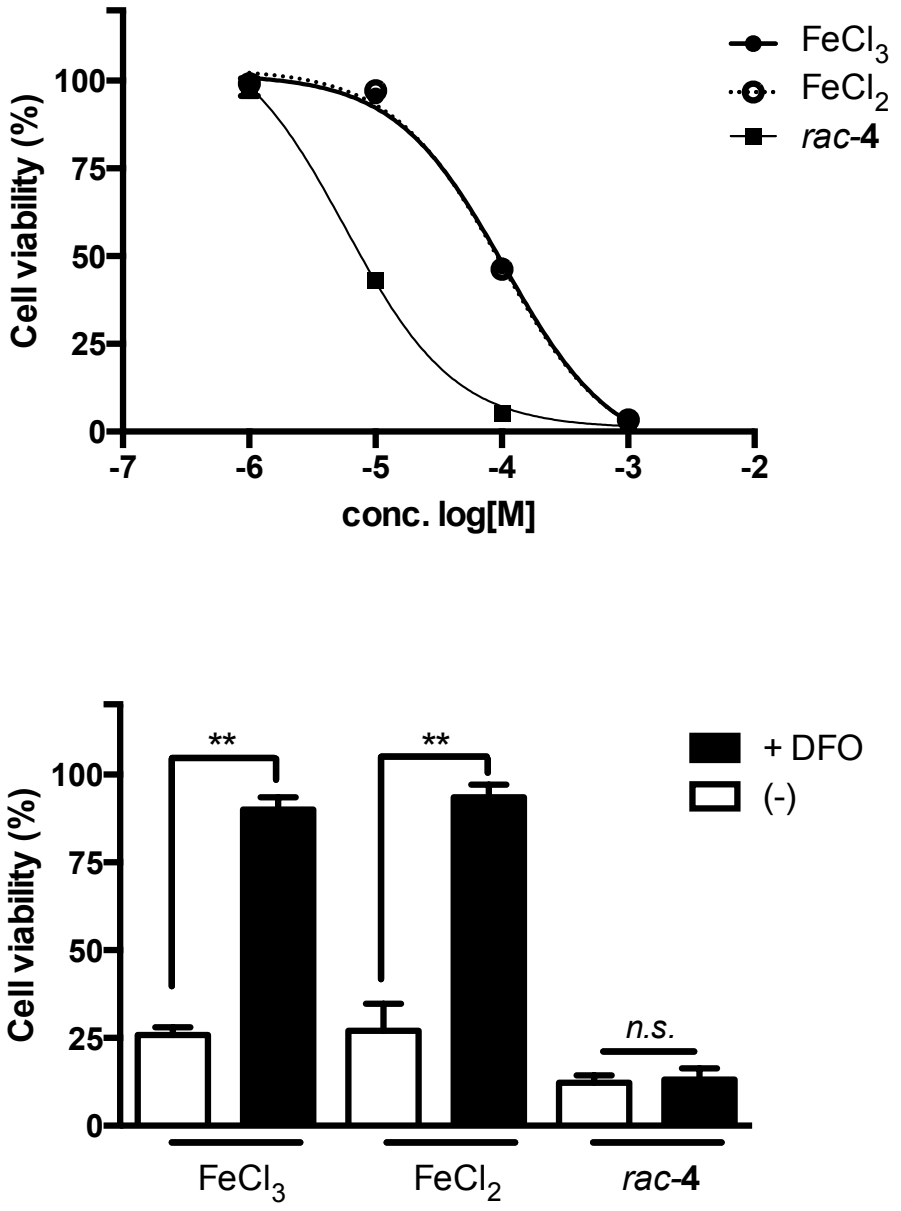

Figure 3.7: Iron-mediated toxicity compared to *rac*-**4** (with or without iron chelator): Serial dilutions of $FeCl_2$ (open circles, dotted line) or $FeCl_3$ (closed circles) and *rac*-**4** (closed squares) were added to HUVEC grown in 96-well plates and toxicity was measured similar as described above (top graph). To test if iron-mediated toxicity was abrogated in the presence of deferoxamine, cells were stimulated with 125 µM of $FeCl_2$, $FeCl_3$ or *rac*-**4** in the presence (filled bars) or absence (open bars) of deferoxamine (80 µM) (bottom graph). The plates were incubated for 24 hours and cell viability was assessed by MTT assay as described. The results of 3 independent experiments are expressed as mean % of cell viability ± SD, relative to the untreated HUVEC. ** $P < 0.01$.

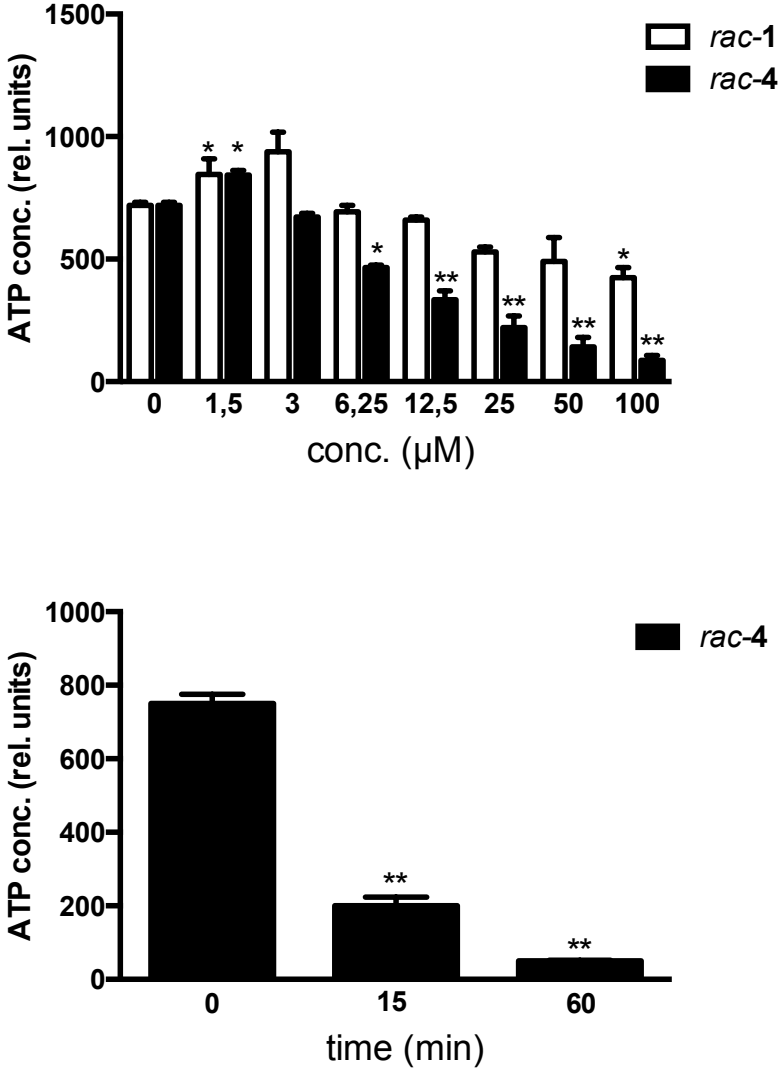

Figure 3.8: Effects on intracellular ATP-levels by *rac*-**1** and *rac*-**4**: HUVEC were grown in 24-well plates until confluence, treated with *rac*-**4** or *rac*-**1** for 24 hours. Subsequently intracellular ATP was measured (top graph). In separate experiments, 50 µM of *rac*-**4** was added to HUVEC and ATP was measured at 0, 15 and 60 minutes after addition of ET-CORM (bottom graph). ATP was measured using an ATP-driven luciferase assay as described in the methods section. The results of 4 independent experiments are expressed as mean relative light units (RLU) ± SD. In all experiments each condition was tested in triplicates. $* P < 0.05$, $** P < 0.01$ vs. the untreated HUVEC.

3.2.2 VCAM-1 inhibition and long term ET-CORM treatment

The previous study has revealed that *rac*-**1** and *rac*-**8** inhibit TNF-α mediated VCAM-1 expression [Romanski et al., 2013]. Also *rac*-**4** inhibits VCAM-1 at low non-toxic concentrations, i.e., [*rac*-**4**] $\leq$ 3 μM (Fig. 3.9). In this study, a more detailed analysis of VCAM-1 inhibition and cell toxicity in long-term experiments is performed only for *rac*-**1** and *rac*-**8**, because they display comparable levels of toxicities and the structural difference between *rac*-**1** and *rac*-**8** is much larger when compared to *rac*-**1** and *rac*-**4**. At 100 μM, cell viability clearly decreased over a time period of 3 days when HUVEC were cultured in the presence of either *rac*-**1** or *rac*-**8** (Fig. 3.10). Since at 50 μM cell viability remained above 95% throughout the culture period, in all long-term cultures for VCAM-1 analysis ET-CORM concentrations were 50 μM or lower. While inhibition of VCAM-1 expression by *rac*-**1** slightly waned in time, VCAM-1 inhibition by *rac*-**8** seems to increase (Fig. 3.11). Inhibition of VCAM-1 expression was also observed for 2-cyclohexenone (**L1**), but not for 1,3-cyclohexanedione (**L2**). To further substantiate that in long-term cultures the inhibitory effect on VCAM-1 expression is much larger for *rac*-**8** as compared to *rac*-**1,** HUVEC were cultured for 5 days in the presence of 25 or 12.5 μM of either *rac*-**1** or *rac*-**8** (Fig. 3.12, top panel). Cell toxicity was not observed under these concentrations (Fig. 3.12, bottom panel). VCAM-1 expression was inhibited by both compounds in a dose-dependent manner, yet, *rac*-**8** was clearly more effective as at both concentrations the inhibitory effect was more pronounced for *rac*-**8**.
The propensity of *rac*-**1** and *rac*-**8** to down-regulate VCAM-1 expression was also present when HUVEC were stimulated with TNF-α one day prior to the addition of these ET-CORMs (Fig. 3.13). However, down-regulation of VCAM-1 expression required the continuous presence of ET-CORM, as VCAM-1 reappeared upon removal of the ET-CORM (Fig. 3.14). In keeping with the notion that for inhibition of VCAM-1 CO needs to be continuously present, current data thus indicate that the difference in kinetic of VCAM-1 inhibition between *rac*-**1** and *rac*-**8** may reflect differences in the amount of intracellular CO.

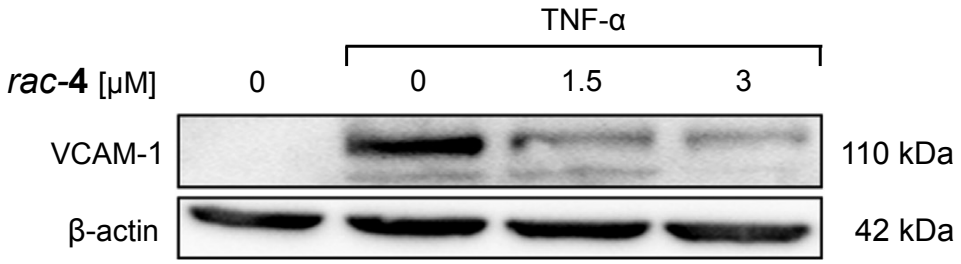

Figure 3.9: Inhibition of VCAM-1 by *rac*-**4** at low concentrations: To demonstrate that *rac*-**4** also inhibits VCAM-1 expression at low, non-toxic concentrations, HUVEC were stimulated with TNF-α for 24 hours in the presence or absence of different concentrations of *rac*-**4**. Note that at these concentrations inhibition of VCAM-1 occurs. VCAM-1 expression was assessed by Western blotting, β-actin was used as loading control.

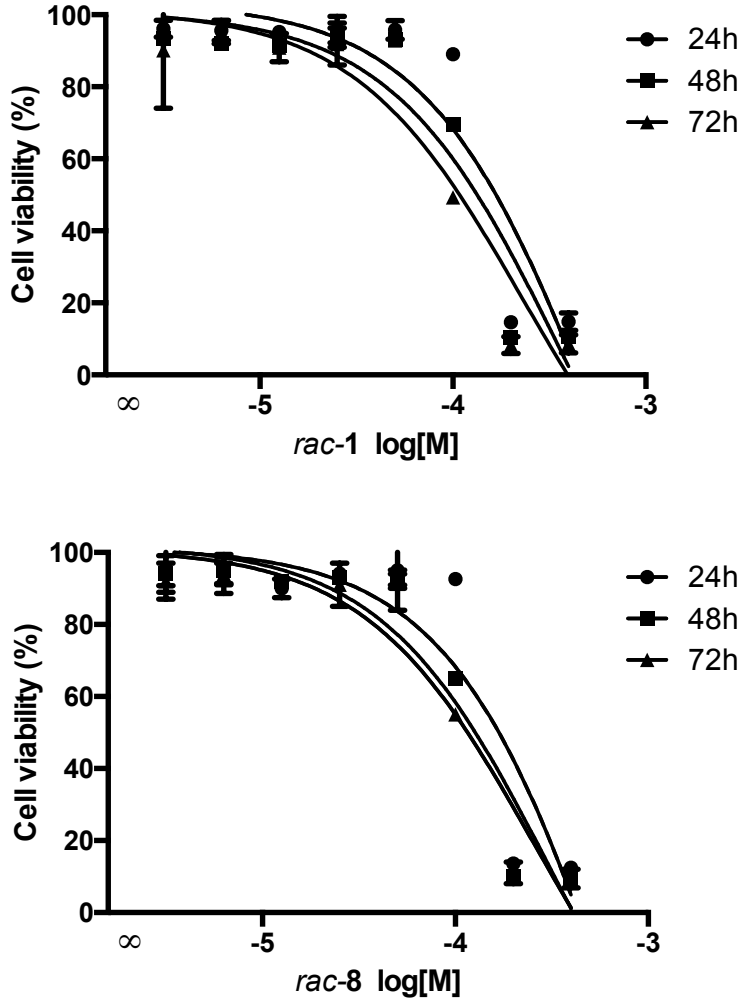

Figure 3.10: Cell viability during long-term treatment with *rac*-**1** and *rac*-**8**: HUVEC were grown in 96-well plates until confluence and subsequently incubated with serial dilutions (0-400 μM) of *rac*-**1** (top graph) or *rac*-**8** (bottom graph). Cell viability was assessed at different time points (24h, 48h and 72h) by MTT assay as described. All experimental conditions were tested in triplicates in at least 5 independent experiments.

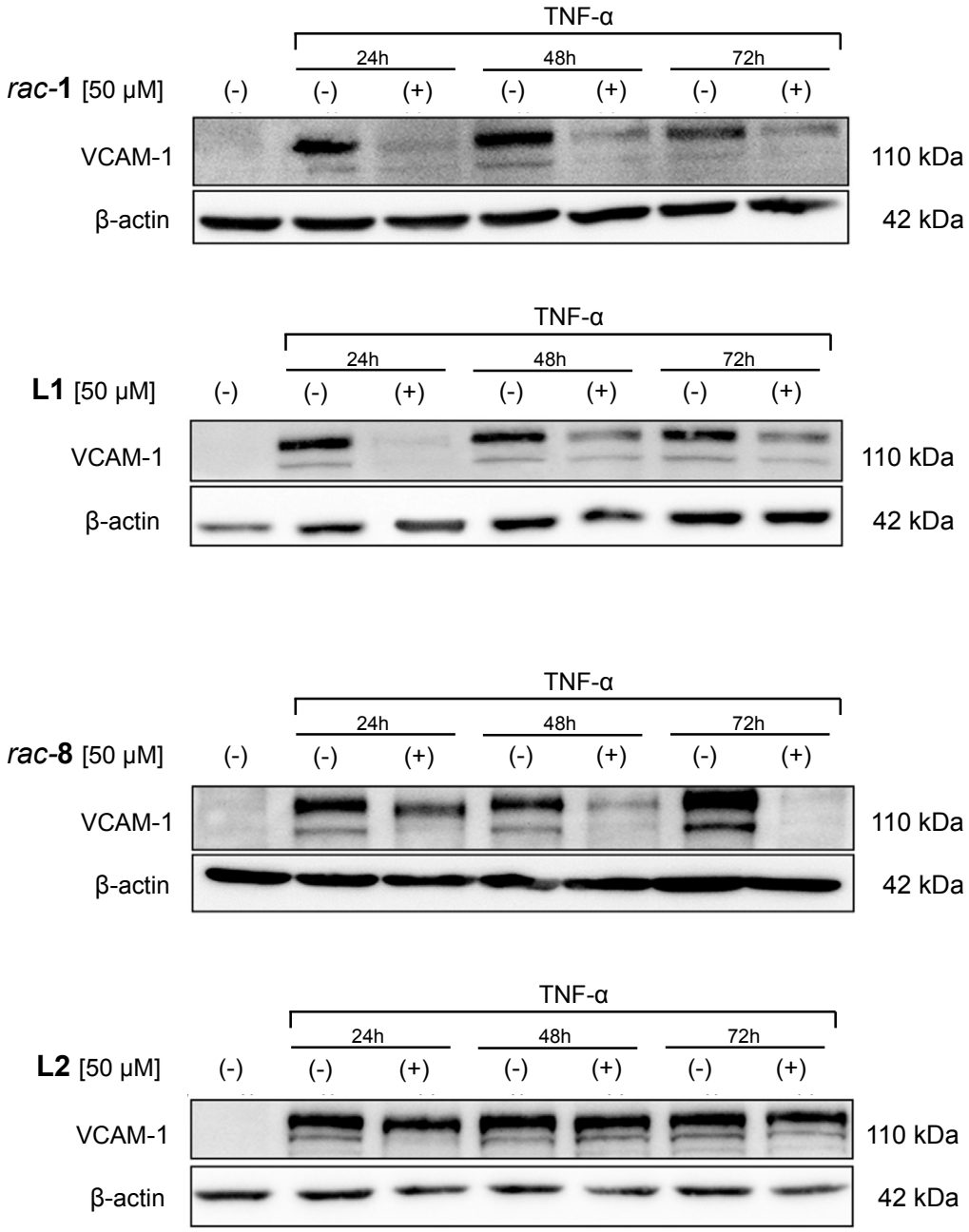

Figure 3.11: Inhibition of VCAM-1 during long-term treatment with ET-CORMs: Cells were stimulated with TNF-α for the indicated time periods in the presence or absence of 50 μM of *rac*-**1**, **L1** (top graphs), *rac*-**8** or **L2** (bottom graphs). Compound **L3** (Fig. 2.2) as an additional possible hydrolysis/disintegration product of *rac*-**8** was tested in various experiments and gave similar results as **L2** (data not shown). Cells that were not stimulated with TNF-α served as control. VCAM-1 expression was assessed by Western blotting; β-actin was used as loading control. Data of a representative experiment are shown. At least 4 independent experiments have been performed.

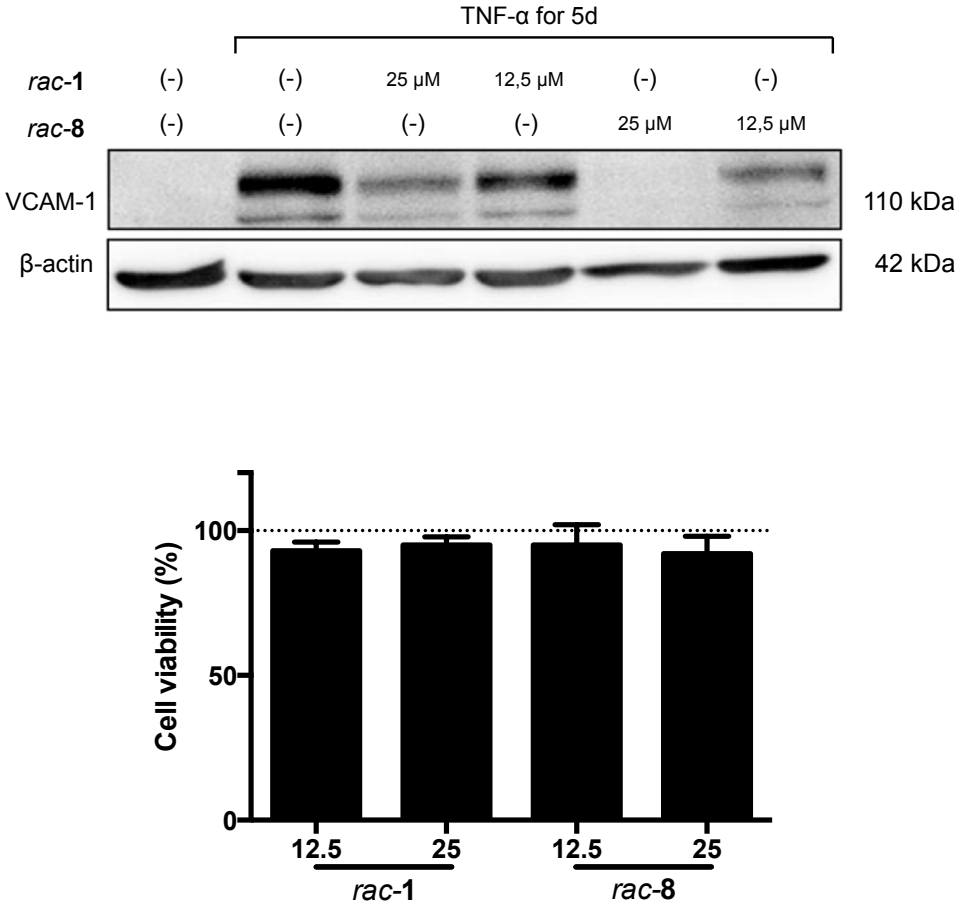

Figure 3.12: Inhibition of VCAM-1 and cytotoxicity after treatment with *rac*-**1** and *rac*-**8** for 5 days: Cells were stimulated with TNF-α for 5 days in the presence or absence of 25 or 12.5 µM of *rac*-**1** or *rac*-**8**. Cells that were not stimulated with TNF-α served as control. VCAM-1 expression was assessed by Western blotting, β-actin was used as loading control (top panel). HUVEC were grown in 96-well plates until confluence and subsequently incubated with 12.5 or 25 µM of *rac*-**1** or *rac*-**8**. Cell viability was assessed by MTT assay (bottom panel) and was expressed as % viable cells relative to the untreated cells. Data of a representative experiment are shown. All experimental conditions were tested in triplicates in at least 5 independent experiments.

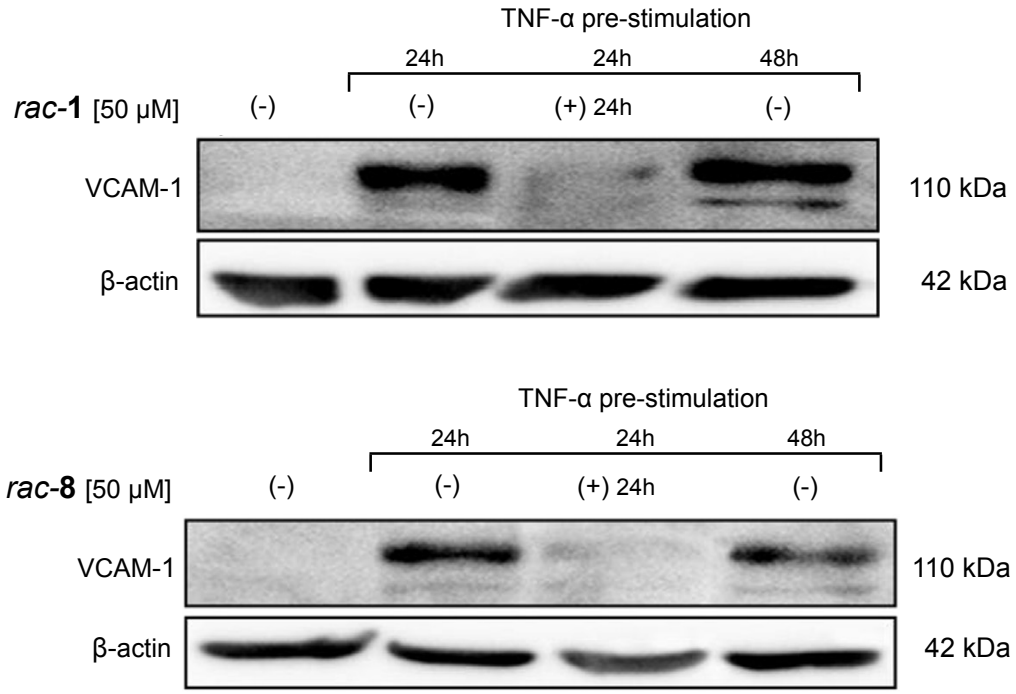

Figure 3.13: Inhibition of VCAM-1 after TNF-α pre-stimulation and treatment with *rac*-**1** and *rac*-**8**: HUVEC were stimulated for 24 hours with TNF-α (10 ng/ml). Hereafter, 50 μM of *rac*-**1** or *rac*-**8** was added without changing the medium and the cells were cultured for additional 24 hours. VCAM-1 expression was assessed at 24 hours of TNF-α stimulation to assure that it was present before addition of *rac*-**1** or *rac*-**8** and after 48h to test if addition of *rac*-**1** or *rac*-**8** was still able to affect VCAM-1 expression. Cells that did not receive *rac*-**1**/*rac*-**8** served as control. Cells that were not stimulated with TNF-α were included to demonstrate VCAM-1 induction. Data of a representative experiment are shown. At least 4 independent experiments have been performed with essentially the same result.

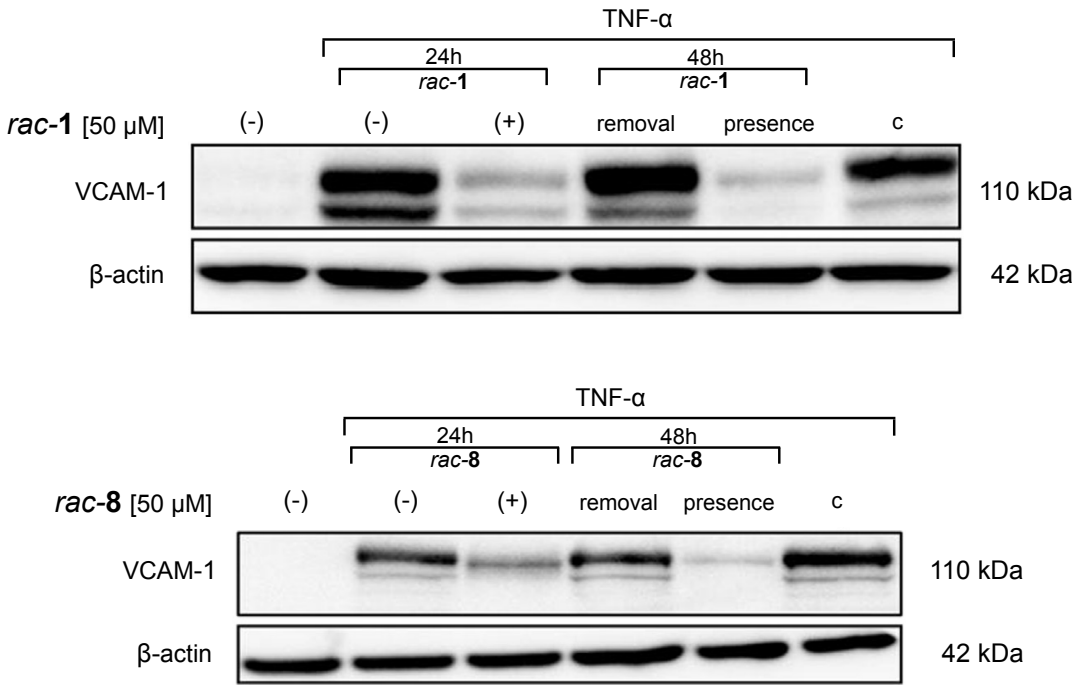

Figure 3.14: Reversible inhibition of VCAM-1 after removal of *rac*-**1** and *rac*-**8**: In separate experiments cells were stimulated for 24 hours with TNF-α (10 ng/ml) in the presence or absence of 50 µM of *rac*-**1** or *rac*-**8**. After 24 hours in separate wells, the medium was exchanged for medium that only contained TNF-α (10 ng/ml) (removal) or medium that contained both TNF-α and *rac*-**1** or *rac*-**8** (presence) and cells were allowed to grow for additional 24 hours. VCAM-1 expression was assessed at 24 hours to demonstrate that *rac*-**1** inhibits VCAM-1 expression and after 48h to demonstrate that VCAM-1 expression reappeared after removal of *rac*-**1** and *rac*-**8** as well. Cell cultures grown for 48h in the continuous presence of TNF-α (c) and cells that were not stimulated with TNF-α were also included. Data of a representative experiment are shown. At least 4 independent experiments have been performed with essentially the same result.

3.2.3 Inhibition of NFκB and activation of Nrf2

In line with inhibition of TNF-α mediated VCAM-1 expression it was found that both *rac*-**1** and *rac*-**8** inhibit NFκB activation as demonstrated by reporter assay. Also 2-cyclohexenone (**L1**), but not 1,3-cyclohexanedione (**L2**), was able to inhibit NFκB (Fig. 3.15). Inhibition of NFκB was not caused by impaired IκBα degradation, in fact, the reappearance of IκBα in the cytoplasm was consistently found to be slightly retarded for both ET-CORMs (Fig. 3.16). Apart from inhibition of NFκB, a significant activation of Nrf2 for both ET-CORMs was also observed (Fig. 3.17, top panel), which was paralleled by the induction of HO-1 at the mRNA- and protein level (Figs. 3.17, bottom panel, and 3.18). Similar as observed for NFκB, only the hydrolysis product of *rac*-**1** but not of *rac*-**8**, affected Nrf2 activation and consequently HO-1 expression.

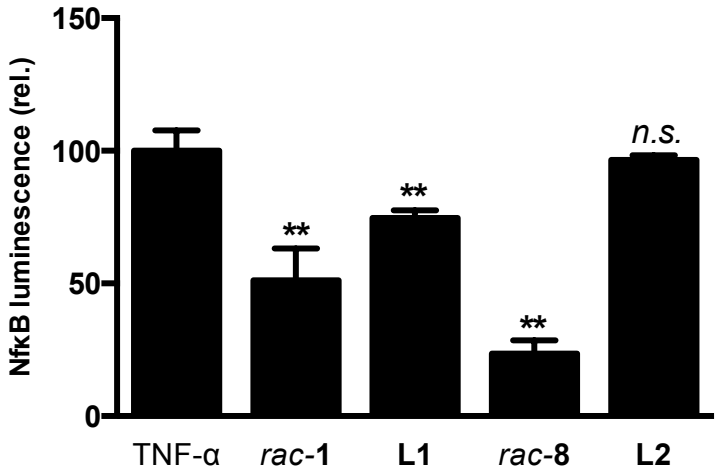

Figure 3.15: Inhibition of NFκB by ET-CORMs: HUVEC were transduced by a lentiviral particle with an inducible promoter construct containing dual NFκB-consensus motifs and with a constitutively active CMV-driven promoter construct both cloned behind luciferase cDNA. Two days after transduction the cells were stimulated for 24 hours with TNF-α (10 ng/ml) in the presence or absence of 50 μM *rac*-**1**, *rac*-**8**, **L1** (2-cyclohexenone) or **L2** (1,3-cyclohexanedione), respectively. Hereafter luciferase expression was measured as described in the methods section. Inducible luciferase expression was normalized for constitutively expressed luciferase to control for differences in transduction efficiency. The data of 4 independent experiments are expressed as mean fold increase ± SD relative to TNF-α stimulated cells. n.s.: not significant, ** $P < 0.01$ vs. TNF-α stimulated cells.

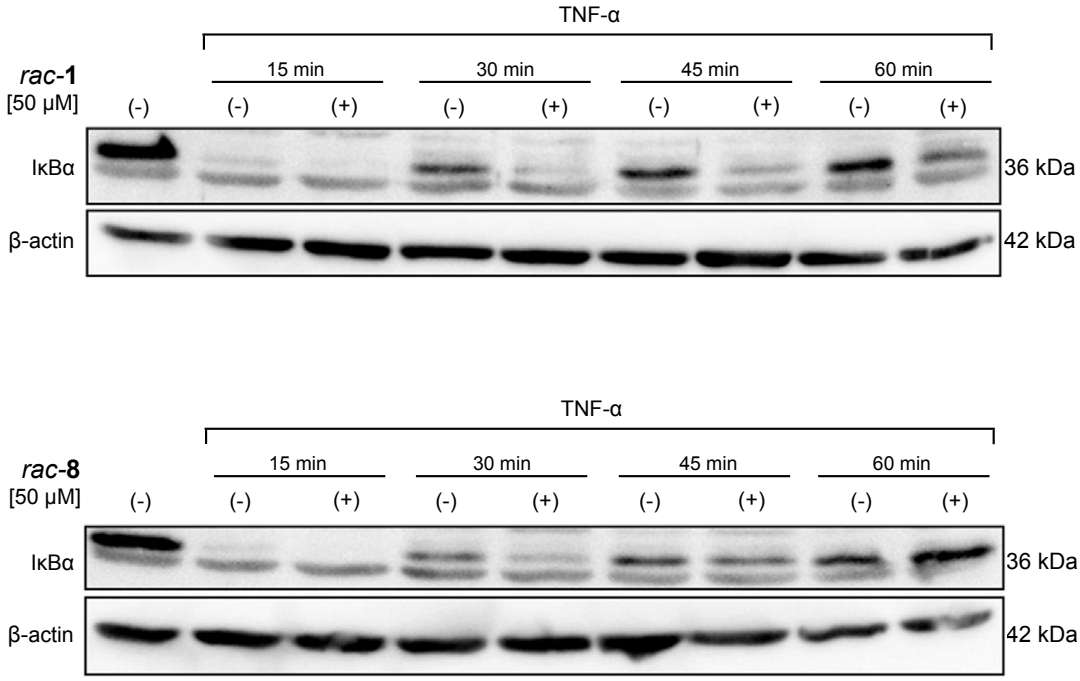

Figure 3.16: IκBα degradation: HUVECs were treated for 4h with 50 μM *rac*-**1** or *rac*-**8** before stimulation with TNF-α. ET-CORMs were present during stimulation. Cell lysates were directly prepared after 15, 30, 45 and 60 minutes of TNF-α stimulation and subjected to electrophoresis and Western blotting for analysis of IκBα expression and β-actin as loading control. Cells that were not stimulated with TNF-α were included to assess constitutive levels of IκBα. The data of a representative experiment is depicted. At least 4 independent experiments have been performed with essentially the same results.

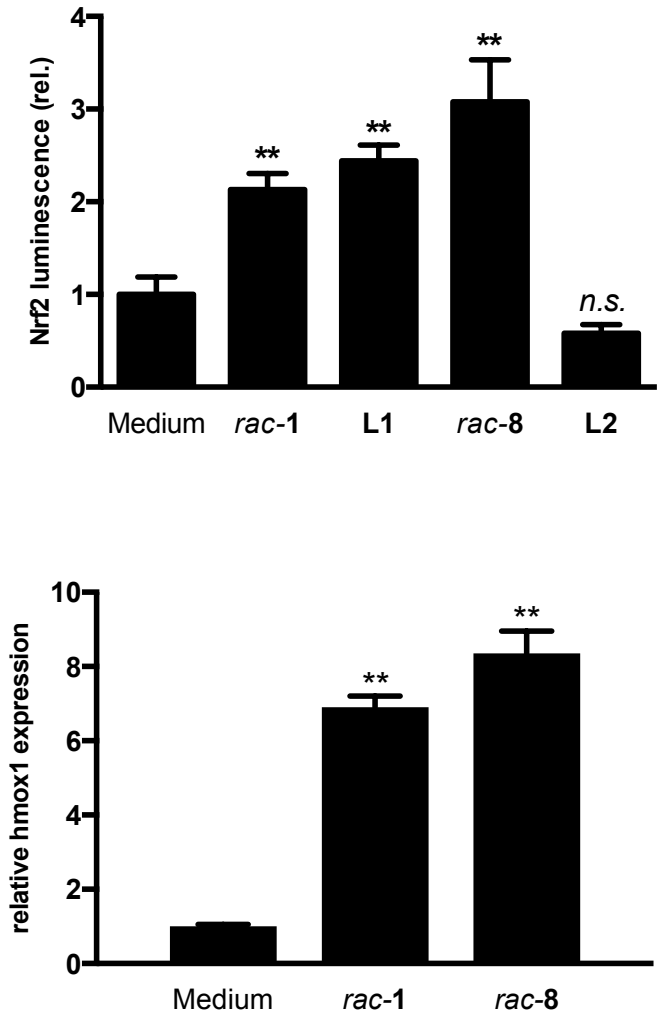

Figure 3.17: Activation of Nrf2 and induction of HO-1 (hmox1) expression by ET-CORMs: **Top:** HUVEC were transduced by a lentiviral particle with an inducible promoter construct containing dual ARE motifs and with a constitutively active CMV-driven promoter construct both cloned behind luciferase cDNA. Two days after transduction the cells were treated for 24 hours with 50 µM *rac*-**1**, *rac*-**8**, **L1** (2-cyclohexenone) or **L2** (1,3-cyclohexanedione) respectively. Hereafter, luciferase expression was measured as described in the methods section. Inducible luciferase expression was normalized for constitutively expressed luciferase to control for differences in transduction efficiency. The data of 4 independent experiments are expressed as mean fold increase ± SD relative to untreated cells (medium). n.s.: not significant, ** $P < 0.01$, vs. untreated cells (medium). **Bottom:** HUVEC were treated for 24 hours with 50 µM *rac*-**1** or *rac*-**8** or left untreated. Hereafter, total RNA was isolated and the expression of HO-1 (hmox1) was quantitated by qPCR and normalized for equal GAPDH expression. Normalized hmox1 mRNA levels are expressed as mean fold increase ± SD relative to untreated cells (medium), ** $P < 0.01$, vs. untreated control.

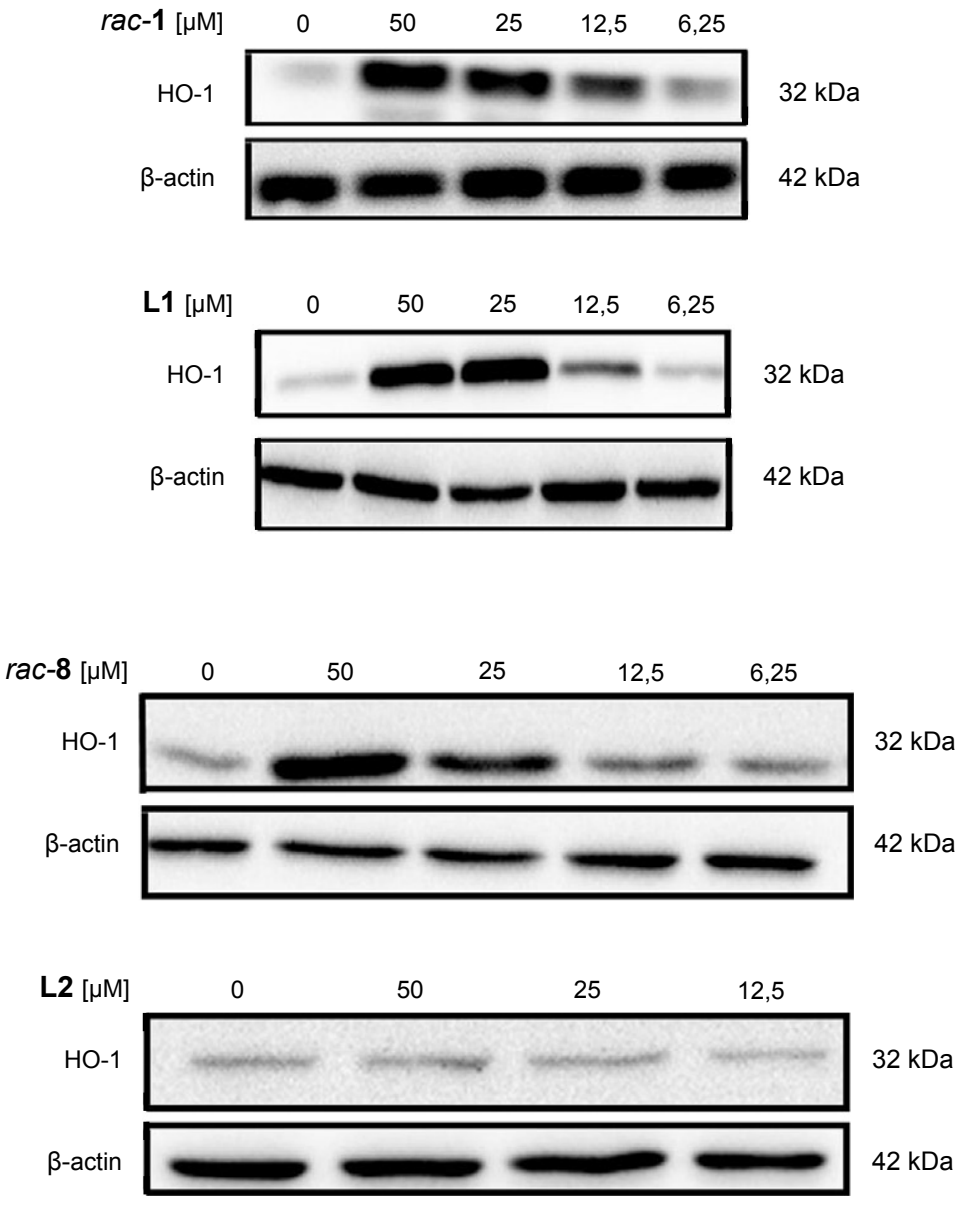

Figure 3.18: Induction of HO-1 expression by ET-CORMs: HUVEC were treated for 24 hours with the indicated concentrations of *rac*-**1**, **L1**, *rac*-**8** or **L2**. Hereafter, protein extracts were made and HO-1 expression was assessed by Western blotting, β-actin was used as loading control. The data of a representative experiment are depicted. At least 4 independent experiments have been performed with essentially the same results.

4
Discussion

Advancing insights in the biological properties of carbon monoxide have clearly changed our way of looking at this class of gasotransmitter: Initially being considered a poisonous gas, recent findings suggest the utilization as a signaling molecule with potential therapeutic effects. Although being the simplest way of application, CO inhalation also threw-up hurdles as it significantly affects the oxygen-carrying capacity of blood. This has pushed CO therapeutic research towards other application modalities and paved the way to design drug molecules that release carbon monoxide in a controllable manner [Motterlini et al., 2005a; Romao et al., 2012; Zobi, 2013]. The mostly utilized CO-releasing molecule, i.e., CORM-3, clearly revealed the therapeutic efficacy in pre-clinical studies. These promising findings lead to the synthesis of enzyme-triggered CORMs that enable for direct intracellular CO release and promise a more specific CO delivery [Romanski et al., 2011a,b].
This dissertation focused on the biological properties of selected ET-CORMs. This study in essence aimed to differentiate if cytotoxicity is mediated by the release of CO and subsequent inhibition of cell respiration or by the concomitant release of iron. The comportment of the biological activity during long-term treatment in terms of reducing pro-inflammatory adhesion molecules was assessed and the involvement of transcription factors in the regulation of VCAM-1 expression was evaluated [Stamellou, Storz et al., 2014]. The relevance of structural alterations for biological efficacy was also studied by using enantiomers of one ET-CORM, the results of which will be discussed first.

4.1 Relevance of structural alterations and biological efficacy of ET-CORM enantiomers

Previous studies on ET-CORMs already showed that structural differences translate into significant changes in biological activity. Accountable for this are differences in the mother compound from which the ET-CORMs are derived, and the type and position of the ester functionality they harbor [Romanski, 2013]. Since this has not been demonstrated for enantiomers, the present study assessed if enantiomers of ET-CORMs (like those that differ structurally) also display differences in their efficacy to mediate a biological response, i.e., cytotoxicity, inhibition of inflammation and protection against cold inflicted cell damage. ET-CORM enantiomers possess the same mother compound and carry the same ester functionality at the same position but differ in the orientation of their functional groups being either in a *trans* or *cis* orientation.

The current data set on cytotoxicity, anti-inflammation (VCAM-1 and HO-1 expression) and cold preservation injury reveals a consistent difference that the biological activity of cis-enantiomers was more pronounced when compared to the trans-enantiomers. In terms of cytotoxicity and anti-inflammatory effects, cis-enantiomers demonstrate efficiency at lower concentrations (25 μM) when compared to trans-enantiomers at higher concentrations (50 μM) (Figs. 3.1 and 3.2). This indicates that lower concentrations of cis-enantiomers have similar cytotoxic effects and similar, if not stronger, anti-inflammatory properties when compared to trans-enantiomers at higher concentrations. Furthermore, with respect to protection against cold inflicted cell damage, the cis-enantiomers were more effective (Fig. 3.3). Within the cis-enantiomers, Stro 790-**C** showed a tendency to be more effective in terms of cytotoxicity and anti-inflammation, while no difference was found in this respect for prevention of cold inflicted injury.
Although these results provide relevant structural information for designing of new ET-CORMs, the underlying reason for the differences between the *cis* and *trans* orientation remains unclear. Differences in cellular uptake and differences in decomposition of the compounds might both play a role.

4.2 Biological activity of ET-CORMs

4.2.1 Intracellular carbon monoxide

After intracellular uptake of ET-CORMs, release of carbon monoxide from the ET-CORMs occurs in two steps. First, esterase-dependent hydrolysis of the ester moiety and, second, oxidative disintegration of the remaining labile enol complex, leading to liberation of carbon monoxide, ferric iron and the corresponding mother compound (Fig. 1.2) [Romanski et al., 2012, 2011a]. Regarding the enzymatic cleavage of ET-CORMs, this study demonstrates that the position of the ester moiety appears to be of crucial importance for CO release and therefore for the efficacy to mediate a particular biological response. The 2-cyclohexenone (**L1**) derived molecules, i.e., *rac*-**1** and *rac*-**4**, unveil a substantial difference in cytotoxicity (Fig. 3.6). Since both compounds have an acetate as ester functionality, a comparison to other 2-cyclohexenone derived ET-CORMs (Fig. 1.1) [Romanski et al., 2013] suggests that their CO releasing characteristics not only emerge from differences in hydrolysis efficiency but may well include the ease of oxidative disintegration. Indeed, the data on CO release by *rac*-**1** and *rac*-**4** (Fig. 3.5) are in line with previous reports that CO release occurs much easier for *rac*-**4** than for *rac*-**1** [Romanski, 2013; Romanski et al., 2012, 2013]. In conclusion, the large difference in cytotoxicity between the 2-cyclohexenone derived ET-CORMs might be explained by the fact that esterase-triggered oxidative disintegration of the *rac*-**4** compound occurs at higher rate when compared to *rac*-**1**.
This study also suggests that the disparity in mediating a biological response is unlikely mediated by differences in cellular uptake of *rac*-**1** and *rac*-**4**. Cyclodextrin formulations, e.g., RAMEB, are frequently used as drug delivery platform for hydrophobic compounds. These bind to the hydrophobic inner-core of the cyclodextrin molecule while the outside of the molecule is hydrophilic, thereby making the complex water soluble. The uptake of the complex now no longer depends on the chemophysical properties of the drug but rather depends on the cyclodextrin carrier. Accordingly, it is expected that for the RAMEB complexes, i.e., RAMEB@*rac*-**1** and RAMEB@*rac*-**4**, it is not the ET-CORMs itself, but the chemical properties of the cyclodextrin formulation that mainly determines the cellular uptake. Yet, the difference in the cytotoxic profile between the two compounds persisted (Fig. 3.6).

Regarding *rac*-**8**, the compound derived from 1,3-cyclohexanedione (**L2**) harbouring two pivalate ester moieties demonstrates a significantly higher cytotoxicity when compared to the mono-acetate and **L1** derived *rac*-**1** [Romanski et al., 2012, 2013]. Previously published data on ester-containing prodrugs suggest pivalate esters to be sterically demanding functionalities in terms of esterase dependent hydrolysis [Shoman et al., 2011; Takahashi et al., 1995]; hydrolysis of *rac*-**8** is therefore expected to be comparably slow. The esterase-dependent hydrolysis of this compound is therefore expected to be comparably slow. Consequentially, this might explain why the levels of toxicity between *rac*-**1** and *rac*-**8** were comparable (Fig. 3.10) despite the fact that *rac*-**8** contains one ester functionality at the outer-position, which, as shown for *rac*-**4**, is in general associated with a faster CO release.
At high and thus toxic concentrations, carbon monoxide is expected to target and bind to intracellular haem-containing proteins [Schatzschneider, 2015], leading to impairment of cell respiration [Sandouka et al., 2005], presumably via inhibition of the mitochondrial cytochrome c oxidase (COX) [Zuckerbraun et al., 2007]. The modulating mechanism of CO on cellular response to stress is only partially understood. However, the data indicating that a decrease in ATP production promotes cell damage further supports the hypothesis that there might be a causal connection between cytotoxicity of ET-CORMs and cellular respiration (Fig. 3.8). Interestingly, the present study demonstrates a significant increase of ATP levels when the cells are treated with ET-CORMs at low concentrations (Fig. 3.8, top graph). This is in concordance with previous studies suggesting that low concentrations of CO application, either gaseous or as CORM-3, lead to increased ATP production. These studies are giving indications that the increase in ATP levels might be mediated by activation of soluble guanyl cyclase (sGC) [Derbyshire and Marletta, 2012; Tsui et al., 2007, 2005] and additionally, that this involves increased enzymatic activity of cytochrome c oxidase (COX, complex IV of the respiratory chain) as well as increased mitochondrial oxygen consumption (state II respiration) indicating an enhancement of oxidative phosphorylation [Almeida et al., 2012; Lo Iacono et al., 2011; Sandouka et al., 2005].
Several studies clearly demonstrate the inhibitory effects of carbon monoxide on the expression of adhesion molecules and its anti-inflammatory modulation *in vitro* and *in vivo* [Caumartin et al., 2011; Katada et al., 2010; Qin et al., 2013; Song et al., 2009]. Carbon monoxide is assumed to induce HO-1, which subsequently may impede the expression of inflammatory mediators [Lee et al., 2006; Seldon et al., 2007]. Consequently, ET-CORMs are able to inhibit VCAM-1 and to induce HO-1 expression, as data of the previous study confirm [Romanski et al., 2013].
In cellular responsiveness to pro-inflammatory stimuli NFκB plays a key role as a rapid acting transcription factor. In the classical (canonical) pathway, NFκB dimers are bound to IκBα in unstimulated cells, which keeps the dimers sequestered and inactive. An inflammatory stimulus, e.g., TNF-α or LPS, induces the degradation of IκBα via signal-induced activation of the IκB kinase (IKK) leading to phosphorylation and subsequent dissociation of IκBα. Furthermore, the phosphorylated IκBα is ubiquitinated and degraded in the proteasome. The released NFκB enters the nucleus, binds to specific DNA-binding sites and induces the transcription of proinflammatory cytokines, chemokines and adhesion molecules, such as VCAM-1 [Gilmore, 2006; Hayden et al., 2006] (Fig. 4.1, left side). The present study demonstrates that ET-CORMs may mediate inhibition of TNF-α-induced VCAM-1 expression via inhibition of NFκB, presumably in an IκBα independent manner (Figs. 3.15 and 3.16).
Another important transcription factor is Nrf2 that controls the expression of antioxidant proteins. Under homeostatic conditions, Nrf2 is bound to Keap1, an adaptor component of a Cul3 (cullin 3)-based ubiquitin E3 ligase complex, which promotes ubiquitination and proteasomal degradation of Nrf2. Oxidative stress, i.e., reactive oxygen species (ROS) and/or GSH depletion, lead to

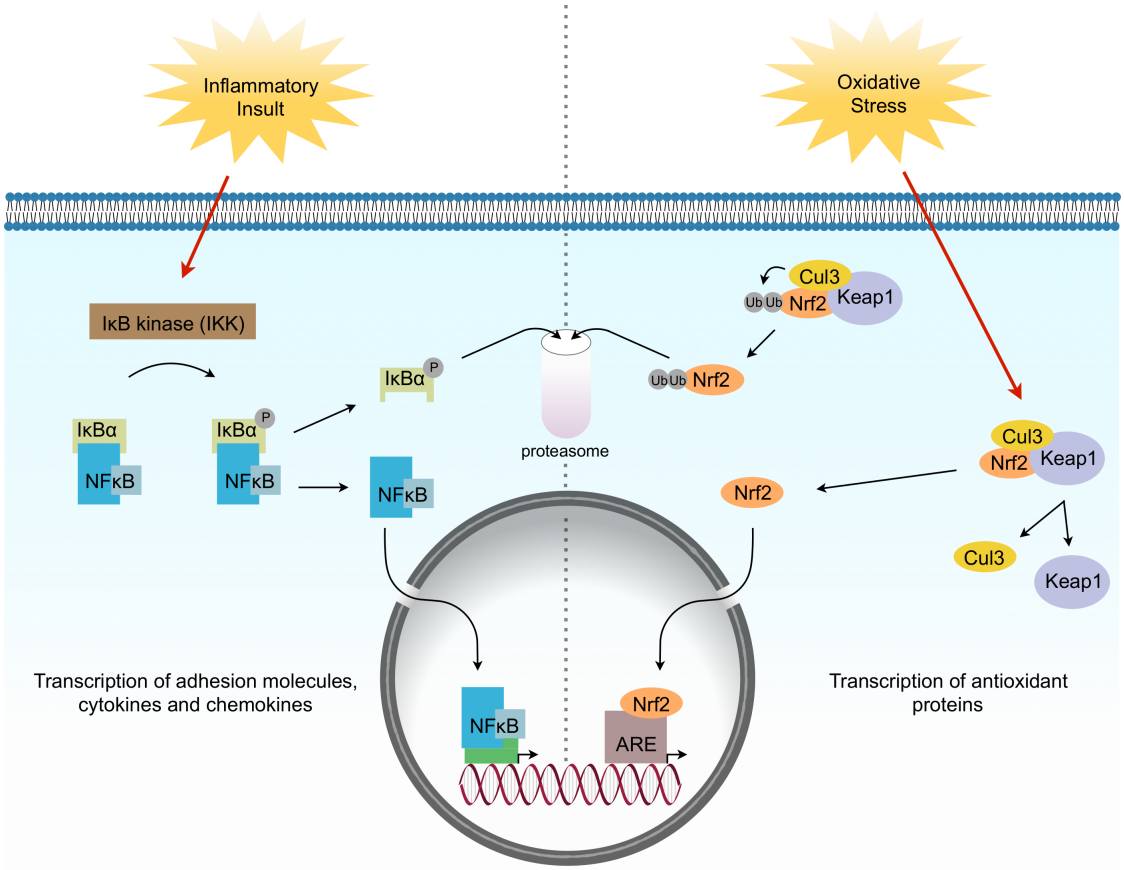

Figure 4.1: Pathways of NFκB and Nrf2: Pathways of NFκB (classical pathway; left side) and Nrf2 (right side; own illustration).

dissociation of the Keap1-Cullin 3 complex, thereby preventing Nrf2 to become ubiquitinated and degraded. In fact, the dissociated Nrf2 now has the propensity to translocate into the nucleus where it binds to the antioxidant response element (ARE) in the promoters of genes encoding anti-oxidative proteins such as HO-1 [Ishii et al., 2000; Ryter and Choi, 2009] (Fig. 4.1, right side). The current data indicates that ET-CORMs can additionally activate Nrf2 (Fig. 3.17). This is in concordance with previously published studies assuming that CO might activate the Nrf2 signaling pathway [Chi et al., 2015; Kim et al., 2011].
Interestingly, there is evidence that ET-CORMs are able to diminish already existing VCAM-1 expression and that the inhibition of VCAM-1 is reversible, once ET-CORMs are removed (Figs. 3.13 and 3.14).
Regarding potential anti-inflammatory effects of the 2-cyclohexenone (**L1**) derived *rac*-**1** and *rac*-**8**, derived from 1,3-cyclohexanedione (**L2**), it could be observed that **L1** but not **L2** inhibits VCAM-1 and induces HO-1, the same applies to inhibition of NFκB and activation of Nrf2. In addition, *rac*-**8** seems to inhibit VCAM-1 slower and in a longer lasting manner when compared to *rac*-**1**. This is in concordance with the previous hypothesis that *rac*-**8** represents a higher resistance to hydrolysis suggesting a slower CO release. An alternative explanation in this case might be the fact that **L1** contributes to VCAM-1 inhibition, whereas **L2** and **L3** do not.

4.2.2 Free intracellular iron

Efficient iron homeostasis, both intracellular and systemic, involves ambitious tasks such as coordination of iron uptake, utilization, and storage to assure adequate supply and to prevent cytotoxicity [Hentze et al., 2010]. Intracellular, the basal level of easy mobilized and redox-active iron is defined as labile cell iron (LCI) or labile iron pool (LIP) [Greenberg and Wintrobe, 1946; Jacobs, 1976]. LCI comprises both Fe^{2+} and Fe^{3+} [Kakhlon and Cabantchik, 2002] and is considered as a transitory and dynamic parameter, which varies with the cellular pH, the redox potential of the medium and the repertoire of substances with chelating moieties [Cabantchik, 2014]. Iron regulatory proteins (IRP) play an important role in controlling intracellular iron homeostasis. In iron-deficient cells IRP inhibit translation of ferritin among other things, whereas high intracellular iron levels promote IRP ubiquitination and degradation, leading to transcription of ferritin [Cairo and Recalcati, 2007; Muckenthaler et al., 2008]. Ferritin itself binds and oxidates ferrous iron (Fe^{2+}) into chemically less reactive ferric iron (Fe^{3+}) [Jacobs et al., 1989], stores the latter and thus limits the generation of toxic radicals.
An excessive rise in LCI however, will lead to compromised cell integrity, mitochondrial iron accumulation and most importantly to catalytic transformation of reactive oxygen intermediates (ROI) to noxious reactive oxygen species (ROS) [Kakhlon and Cabantchik, 2002; Kruszewski, 2003]. Products of this Fenton reaction, such as hydroxyl radicals, lead to oxidative stress [Kruszewski, 2004]. Once the intracellular antioxidant buffer is depleted, the imbalance will lead to cell damage [Kruszewski, 2003; Muckenthaler et al., 2008]. Interestingly, oxidative stress induces haem oxygenase-1 (HO-1) [Applegate et al., 1991], which itself further induces ferritin [Balla et al., 1992; Gonzales et al., 2002] and inhibits apoptosis by regulating cellular prooxidant iron [Brouard et al., 2000; Otterbein and Choi, 2000].
In contrast to liberated ferrous iron (Fe^{2+}) during degradation of haem or cellular distribution of iron through transferrin, ET-CORMs distribute ferric iron, i.e., Fe^{3+}, the chemically less reactive form. Since iron homeostasis needs to be strictly maintained the fate of the concomitantly released Fe^{3+} needs to be addressed, as this may also jeopardize iron homeostasis. It is unlikely that the released Fe^{3+} contributes to cell toxicity of ET-CORMs as toxicity for $FeCl_2$ or $FeCl_3$ was observed at much higher concentration as compared to *rac*-**4** (Fig. 3.7, top graph). Additionally, iron chelators abrogated $FeCl_2$/$FeCl_3$-mediated toxicity, whereas this was not observed for *rac*-**4** (Fig. 3.7, bottom graph). It is assumed that the released ferric iron may lead to induction of ferritin, thus preparing the cells to scavenge potential redox substrates, e.g., Fe^{2+}.

4.2.3 The role of the mother compound

As demonstrated in this study, 2-cyclohexenone (**L1**), the mother compound of *rac*-**1** and *rac*-**4**, liberated during ET-CORM cleavage contributes to the bioactivity of the latter. **L1** activates Nrf2 (Fig. 3.17), and inhibits VCAM-1 expression (Fig. 3.11, top graphs) most likely via inhibition of NFκB. In contrast to *rac*-**1** and *rac*-**4**, **L1** was neither cytotoxic nor was it able to protect cells against cold preservation injury [Romanski et al., 2013]. The current data suggests that released CO and the hydrolysis product **L1** may act in a synergistic or complementary manner. Hence, ET-CORMs might be considered as bifunctional, i.e., they can release two functional mediators. For the other gasotransmitter, i.e., NO and H_2S, bifunctional gasotransmitter-based complexes have already been reported: The so-called cyclooxygenase inhibiting nitric oxide donors (CINODs) and H_2S-releasing NSAIDs [Fiorucci and Distrutti, 2011]. NO-naproxen (Naproxcinod), for instance, is a nitrosylated naproxen derivative with the ability to release nitric oxide (NO)

[Cicala et al., 2000], which was already investigated in clinical trials [White et al., 2011]. As for hydrogen sulfide, there are complexes available that contain H_2S-releasing groups on naproxen and diclofenac respectively, i.e., ATB-346 and ATB-337, which are investigated *in vivo* [Campolo et al., 2013; Dief et al., 2015; Herrera et al., 2015; Wallace et al., 2010, 2007]. With respect to *rac*-**8**, the mother compound, i.e., 1,3-cyclohexanedione (**L2**) or the enol pivalate (**L3**) (Fig. 2.2) show neither effects on cytotoxicity [Romanski, 2013], VCAM-1 inhibition (Fig. 3.11, bottom graphs and Fig. 3.15) and HO-1 induction (Figs. 3.17 and 3.18), nor protection against cold preservation injury (data not shown). Hence it is most likely, that the bioactivity of *rac*-**8** evokes primarily by the release of CO.

5
Limitations and Future Prospects

Enzyme-triggered CO-releasing molecules pursue the seminal feasibility of tissue-targeted CO delivery. It has to be admitted that intracellular esterases are ubiquitous therefore CO delivery with true tissue-specificity is not guaranteed with the current ET-CORMs. Thus, currently available ET-CORMs need to be structurally optimized to be cleaved by either esterase subforms or tissue-specific enzymes to aim for cell restricted CO release.
In fact, so-called protease-triggered CORMs have been developed and implemented in *in vitro* experiments [Sitnikov et al., 2015]. These compounds are designed as oxydiene-Fe$(CO)_3$ complexes with a peptide sequence as a side chain that is cleaved by penicillin G amidase (PGA). PGA-induced release of CO showed inhibition of VCAM-1 expression and induction of HO-1 in HUVEC [Sitnikov et al., 2015]. Admittedly, further exploration is necessary, although this promising data serves as a fundament to design ET-CORMs cleaved by tissue-specific proteases. Furthermore, ET-CORMs may be linked to a vector for cell-specific intracellular uptake. Similarly to the cyclodextrin formulation, this vector would act as a smart coat pharmaceutical or a specific carrier conjugate that could transfer the compound to a particular tissue. A potential vector might be bile acid, which can only be absorbed by specific cells, i.e., hepatocytes or enterocytes, showing particular bile acid transporters. Zobi *et al.* addressed to the problem of cellular internalization with conjugation of photoCORM to vitamin B_{12}. Cyanocobalamin (B_{12}) is used as a water-soluble vector to transport photoCORM into nonspecific cells, following photolysis [Zobi et al., 2013]. Similarly, Mede *et al.* modified manganese(I)-based photoCORMs that are enzymatically transformed inside of cells to trap the complexes and to ensure intracellular photo-triggered release of carbon monoxide [Mede et al., 2018].
The principle of conjugating CORMs to a vector is currently investigated within several studies. CORMs have been synthesized with various carriers such as proteins, nanoparticles and micelles to ameliorate stability and kinetics [Garcia-Gallego and Bernardes, 2014; Inaba et al., 2015; Kautz et al., 2016].
In the last years fluorescent sensors were introduced to detect CO release in living cells. A CO sensor (COSer) is a genetically encoded fluorescent probe with the need to be transfected into cells [Wang et al., 2012], whereas CO-Probe 1 (COP-1) is a chemical reagent that interacts with carbon monoxide to trigger a fluorescent reaction [Michel et al., 2012]. In this study COP-1 was used to evaluate the speed and extent of intracellular CO release. As demonstrated, it was possible to evaluate CO liberation. However, difficulties evolved from a high background fluorescence signal of COP-1.
Promising new fluorescent CO detectors have been presented most recently holding the advantage of detecting even endogenous CO generation over the well-known COSer and COP-1 [Feng

et al., 2016; Li et al., 2016]. Further research and technical advances of the probes are necessary to visualize intracellular levels of carbon monoxide in order to assess its biological activities and signaling effects.
To this day, it has been complicated to specify chemical components of LCI [Cabantchik, 2014] and to describe the role of changes in iron metabolism during inflammation and interactions between inflamed tissue and cells of the immune system [Hentze et al., 2010]. Within this study, ET-CORMs were additionally evaluated using a Phen Green Assay (Thermo Fisher Scientific). The assembled data showed no reproducibility, and neither dynamic tracing nor evaluation of the potency of ferric iron release were possible (data not shown). There is not only a necessity to determine the dynamic parameter LCI in living cells but also to observe the intracellular (and systemic) iron homeostasis with the help of novel metallosensors.
This study demonstrates that, first, ET-CORMs inhibit VCAM-1 expression, potentially reducing leukocyte adhesion and diapedesis, and, second, presumably induce HO-1 in an independent manner. This is in concordance with previous studies showing inhibition of production of inflammatory cytokines in LPS-stimulated macrophages [Otterbein et al., 2000; Sawle et al., 2005] and possibly modulation of initiation of immune responses [Otterbein et al., 2003a] after administration of CO. Alternative studies demonstrate a reduction of infiltration of T cells, leukocytes and macrophages in transplant recipients of aortic grafts after CO inhalation [Otterbein et al., 2003b]. Focused on the acquired immune system, upregulation of HO-1 and therefore endogenous production of CO was proposed to influence the function of $CD4^+CD25^+$ regulatory T cells in immunosuppression [Brusko et al., 2005].
To evaluate if ET-CORMs show modulatory effects on the acquired immune system, naive $CD4^+$ T cells isolated from PBMC were used to conduct the MTT cell toxicity assay and ^{3}H-thymidine incorporation assay. While MTT cell toxicity assay showed similar results in terms of cytotoxicity when compared to experiments with HUVEC, ^{3}H-thymidine incorporation assay with different ET-CORMs using concentrations of 25 µM to 100 µM showed no clear effect on proliferation of naive $CD4^+$ T cells, neither definite inhibition nor stimulation when compared to positive or negative control (data not shown). The inconclusive results and the lack of data on the effects of CO or CORMs especially on $CD4^+$ T cells need continuative attention since modulation of the adaptive immune system could be another interesting quality of ET-CORMs in terms of reduction of graft versus host reactions and graft rejection in transplant recipients.
Despite the beneficial effects of **L1**, little is known about the intracellular interactions, the systemic metabolism and the biological relevance of the mother compounds, i.e., **L1** as well as **L2** and **L3**. As soon as ET-CORMs are further evaluated *in vivo*, this might lead to profound knowledge of this issue. Simultaneously, our findings imply the intriguing opportunity to further design and optimize ET-CORMs as bifunctional complexes.
As demonstrated in this study, this is partially already in existence. The 2-cyclohexenone (**L1**) derived ET-CORMs, i.e., *rac*-**1** and *rac*-**4** can act as bifunctional complexes in a way that the by-products summate the beneficial outcome in terms of VCAM-1 inhibition and induction of HO-1. The design of bifunctional gasotransmitter-based molecules has been reported for NO and H_2S, as described before. The principle behind bifunctional compounds regarding synergistic and complementary products is very interesting and intriguing. Several *in vivo* studies imply a protective effect of CO in inflammatory bowel disease [Takagi et al., 2015], mostly by regulation of intestinal inflammation [Babu et al., 2015b]. Combining ET-CORMs with conventional pharmaceuticals to design bifunctional carbon monoxide-based complexes, e.g., for topical application in inflammatory bowel disease or inflammatory diseases of the skin, would be an ambitious approach opening numerous opportunities.

In fact, it has already been demonstrated that this approach is feasible by introducing novel methyl fumarate-derived compounds (FumET-CORMs). Dimethyl fumarate is used as a treatment in psoriasis and multiple sclerosis and is known as a strong anti-inflammatory agent. Hence, Bauer *et al.* combined the anti-inflammatory effects of dimethyl fumarate and ET-CORMs to synthesize the bifunctional FumET-CORMs. It could be demonstrated that combined synergistic anti-inflammatory effects of FumET-CORMs are more pronounced compared to each compound on its own, especially compared to the clinically used dimethyl fumarate [Bauer et al., 2017].
Further promising approaches are Oral Carbon Monoxide Release Systems (OCORS). Steiger *et al.* introduced a localized and controlled oral drug delivery of carbon monoxide *in vitro* and *in vivo*. Therefore, ruthenium-containing CORM-2 was formulated to micro scale OCORS (M-OCORS) demonstrating preventive effects in chemically induced colitis in mice. In addition, the scientists introduced the principle of enzyme-triggered Oral Carbon Monoxide Release Systems (E-OCORS) formulating ET-CORM/RAMEB complexes for oral administration [Steiger et al., 2016].

6
Conclusion

In this work a comprehensive investigation of selected ET-CORMs with respect to their biological activity was conducted [Stamellou, Storz et al., 2014]. The chemical design of ET-CORMs holds particular advantages over present forms of CO application. CO inhalation and other CORMs predominantly deliver CO via unspecific passive diffusion to cells or tissue, whereas ET-CORM release CO only intracellularly in an esterase dependent manner. When compared to existing CORMs, e.g., frequently used CORM-3, lower concentrations of ET-CORMs can be applied to cells to achieve similar biological activities. Although a direct comparison between ET-CORMs and CORM-3 was not yet performed, this study demonstrates complete inhibition of VCAM-1 expression at 50 μM of *rac*-**1** (Fig. 3.11) and at 3 μM of *rac*-**4** (Fig. 3.9). On the contrary, for CORM-3, 1 mM has been required to completely inhibit TNF-α mediated VCAM-1 expression [Song et al., 2009]. This study revealed clear indication that the cytotoxic effect of ET-CORMs particularly depends on the release of CO, i.e., the speed or extent of CO release, for the following reasons. Firstly, the disparity in cytotoxicity is unlikely due to differences in cellular uptake as cyclodextrin formulated ET-CORMs indicate (Fig. 3.6). Secondly, the mother compounds itself, i.e., **L1**, **L2** and **L3** show no cytotoxic effect [Romanski et al., 2013]. Thirdly, there is no indication that released ferric iron contributes noticeably to the cytotoxic effect, since cytotoxicity was observed at a much higher concentration using $FeCl_2$ and $FeCl_3$ (Fig. 3.7, top graph). Additionally, iron chelators were able to abrogate toxic effects of $FeCl_2$ and $FeCl_3$, whereas cytotoxicity of *rac*-**4** persisted (Fig. 3.7, bottom graph). Fourthly, the data further supports the hypothesis that there might be a causal connection between impairment of cellular respiration and cytotoxicity of ET-CORMs via release of CO (Fig. 3.8). This thesis also demonstrated that ET-CORMs effectively inhibit the expression of VCAM-1 upon TNF-α stimulation. During long-term treatment, *rac*-**8** appears to inhibit VCAM-1 in a slower and longer lasting manner when compared to *rac*-**1**. ET-CORMs may mediate the inhibition of NFκB, presumably in an IκBα independent manner, and activate the antioxidant Nrf2 pathway, leading to induction of HO-1. Regarding the mother compounds 2-cyclohexenone (**L1**) and 1,3-cyclohexanedione (**L2**), it could be observed that **L1** but not **L2** inhibits VCAM-1 and induces HO-1, the same applies to inhibition of NFκB and activation of Nrf2. In this matter, there might be a summation of beneficial properties in 2-cyclohexenone derived ET-CORMs. Finally, the findings on ET-CORM enantiomers may furthermore help designing favorable ET-CORMs with improved bioactivity. In addition to the different possibilities in structural optimization of ET-CORMs, the current work warrants *in vivo* studies. Ultimately, this may lead to the development of novel pharmaceuticals that deliver carbon monoxide in a highly tissue-specific manner to overcome side effects and to focus the therapeutic effects to organs where they are most needed.

7
Summary

Carbon monoxide (CO) is an ambivalent gasotransmitter endogenously generated during physiological degradation of haem. While being highly toxic at elevated concentrations, the gaseous molecule holds promising properties at low and physiological concentrations. Application of the exogenous equivalent can mimic these beneficial characteristics including cytoprotective and anti-proliferative effects as well as anti-inflammatory properties.
Enzyme-triggered CO-releasing molecules (ET-CORMs) are a novel class of transition metal carbonyl complexes that offer several advantages over previous forms of exogenous CO application. While inhalation of CO and other CORMs predominantly deliver carbon monoxide via unspecific passive diffusion to cells or tissue, ET-CORMs allow for an intracellular administration of carbon monoxide. More precisely, esterase dependent, enzymatic cleavage of the chemical bonds leads to intracellular release of carbon monoxide, ferric iron and the mother compound. Previously published data demonstrates that the biological properties of ET-CORMs strongly depend on their chemical structure, the type and position of the ester substituent as well as the mother compound from which they are derived.
In this work a series of structurally different ET-CORMs (*rac*-**1**, *rac*-**4** and *rac*-**8**) were investigated in human umbilical vein endothelial cells: The data showed that the cytotoxic effect of ET-CORMs relies on the speed or extent of carbon monoxide release. The disparity in cytotoxicity is unlikely to be mediated by different intracellular uptake of the investigated compounds based on the notion that the cellular uptake of the purpose-built cyclodextrin encapsulated ET-CORMs is equal and the cytotoxic profile remained unaltered. At toxic concentrations, there was no indication that released ferric iron or the mother compounds contribute noticeably to the cytotoxic effect of ET-CORMs. In this case (i.e., toxic concentrations of CO), it is expected that CO binds to intracellular haem containing proteins leading to an impairment of cell respiration. The collected data demonstrates that ATP depletion promotes cell damage, thus supporting the hypothesis of a causal connection between the cytotoxicity of ET-CORMs and cellular respiration. On the contrary, treatment with ET-CORMs at low concentrations significantly increases intracellular ATP levels. This is in agreement with previous studies on exogenous CO application suggesting that the increase in ATP levels might be mediated by activation of soluble guanyl cyclase, which in turn indicates an enhancement in oxidative phosphorylation.
In terms of anti-inflammatory modulation, the investigated ET-CORMs effectively inhibited TNF-α induced VCAM-1 expression and may mediate the inhibition of VCAM-1 via inhibition of NFκB, presumably in an IκBα independent manner. Additionally, ET-CORMs showed activation of the Nrf2 signaling pathway leading to induction of the antioxidant protein HO-1. It is well

known that both the NFκB and Nrf2 signaling pathway are crucial for the cellular response and regulation to inflammatory stimuli.
The mother compound of *rac*-**1** and *rac*-**4** itself, i.e., 2-cyclohexenone (**L1**), inhibited VCAM-1 and induced HO-1 expression. Accordingly, **L1**-derived ET-CORMs can act as bifunctional complexes in a way that the beneficial effects of the by-products summate. This opens up various opportunities for the complementary delivery of ET-CORMs and a second agent.
Finally, enantiomers of ET-CORMs displayed differences in the efficacy to mediate a biological response, providing essential structural information. Cis-enantiomers showed a pronounced biological activity in terms of cytotoxicity, anti-inflammation and cold preservation injury when compared to trans-enantiomers. This information can be employed to chemically modify and thus optimize existing ET-CORMs.
Although intracellular esterases are ubiquitous and tissue-targeted delivery of CO based on ET-CORMs cannot be guaranteed at this point, this work set a first foundation on the road to tissue-specific delivery of carbon monoxide generating fundamental insights for designing ET-CORMs with differential CO release and biological activities.

List of Figures

List of Tables

Bibliography

Alberto, R. and Motterlini, R. (2007). Chemistry and biological activities of co-releasing molecules (corms) and transition metal complexes. *Dalton Trans*, (17):1651–60.

Almeida, A. S., Queiroga, C. S., Sousa, M. F., Alves, P. M., and Vieira, H. L. (2012). Carbon monoxide modulates apoptosis by reinforcing oxidative metabolism in astrocytes: role of bcl-2. *J Biol Chem*, 287(14):10761–70.

Applegate, L. A., Luscher, P., and Tyrrell, R. M. (1991). Induction of heme oxygenase: a general response to oxidant stress in cultured mammalian cells. *Cancer Res*, 51(3):974–8.

Babu, D., Leclercq, G., Goossens, V., Remijsen, Q., Vandenabeele, P., Motterlini, R., and Lefebvre, R. A. (2015a). Antioxidant potential of corm-a1 and resveratrol during tnf-alpha/cycloheximide-induced oxidative stress and apoptosis in murine intestinal epithelial mode-k cells. *Toxicol Appl Pharmacol*.

Babu, D., Motterlini, R., and Lefebvre, R. A. (2015b). Co and co-releasing molecules (co-rms) in acute gastrointestinal inflammation. *Br J Pharmacol*, 172(6):1557–73.

Balla, G., Jacob, H. S., Balla, J., Rosenberg, M., Nath, K., Apple, F., Eaton, J. W., and Vercellotti, G. M. (1992). Ferritin: a cytoprotective antioxidant strategem of endothelium. *J Biol Chem*, 267(25):18148–53.

Bathoorn, E., Slebos, D. J., Postma, D. S., Koeter, G. H., van Oosterhout, A. J., van der Toorn, M., Boezen, H. M., and Kerstjens, H. A. (2007). Anti-inflammatory effects of inhaled carbon monoxide in patients with copd: a pilot study. *Eur Respir J*, 30(6):1131–7.

Bauer, B., Goderz, A. L., Braumuller, H., Neudorfl, J. M., Rocken, M., Wieder, T., and Schmalz, H. G. (2017). Methyl fumarate-derived iron carbonyl complexes (fumet-corms) as powerful anti-inflammatory agents. *ChemMedChem*, 12(23):1927–1930.

Bauer, I. and Pannen, B. H. (2009). Bench-to-bedside review: Carbon monoxide–from mitochondrial poisoning to therapeutic use. *Crit Care*, 13(4):220.

Bergstraesser, C., Hoeger, S., Song, H., Ermantraut, L., Hottenrot, M., Czymai, T., Schmidt, M., Goebeler, M., Ponelies, N., Stich, C., Loesel, R., Molema, G., Seelen, M., van Son, W., Yard, B. A., and Rafat, N. (2012). Inhibition of vcam-1 expression in endothelial cells by corm-3: the role of the ubiquitin-proteasome system, p38, and mitochondrial respiration. *Free Radic Biol Med*, 52(4):794–802.

Bradford, M. M. (1976). A rapid and sensitive method for the quantitation of microgram quantities of protein utilizing the principle of protein-dye binding. *Anal Biochem*, 72:248–54.

Brouard, S., Otterbein, L. E., Anrather, J., Tobiasch, E., Bach, F. H., Choi, A. M., and Soares, M. P. (2000). Carbon monoxide generated by heme oxygenase 1 suppresses endothelial cell apoptosis. *J Exp Med*, 192(7):1015–26.

Brusko, T. M., Wasserfall, C. H., Agarwal, A., Kapturczak, M. H., and Atkinson, M. A. (2005). An integral role for heme oxygenase-1 and carbon monoxide in maintaining peripheral tolerance by cd4+cd25+ regulatory t cells. *J Immunol*, 174(9):5181–6.

Cabantchik, Z. I. (2014). Labile iron in cells and body fluids: physiology, pathology, and pharmacology. *Front Pharmacol*, 5:45.

Cairo, G. and Recalcati, S. (2007). Iron-regulatory proteins: molecular biology and pathophysiological implications. *Expert Rev Mol Med*, 9(33):1–13.

Campolo, M., Esposito, E., Ahmad, A., Di Paola, R., Wallace, J. L., and Cuzzocrea, S. (2013). A hydrogen sulfide-releasing cyclooxygenase inhibitor markedly accelerates recovery from experimental spinal cord injury. *FASEB J*, 27(11):4489–99.

Caumartin, Y., Stephen, J., Deng, J. P., Lian, D., Lan, Z., Liu, W., Garcia, B., Jevnikar, A. M., Wang, H., Cepinskas, G., and Luke, P. P. (2011). Carbon monoxide-releasing molecules protect against ischemia-reperfusion injury during kidney transplantation. *Kidney Int*, 79(10):1080–9.

Chi, P. L., Lin, C. C., Chen, Y. W., Hsiao, L. D., and Yang, C. M. (2015). Co induces nrf2-dependent heme oxygenase-1 transcription by cooperating with sp1 and c-jun in rat brain astrocytes. *Mol Neurobiol*, 52(1):277–92.

Cicala, C., Ianaro, A., Fiorucci, S., Calignano, A., Bucci, M., Gerli, R., Santucci, L., Wallace, J. L., and Cirino, G. (2000). No-naproxen modulates inflammation, nociception and downregulates t cell response in rat freund's adjuvant arthritis. *Br J Pharmacol*, 130(6):1399–405.

Coburn, R. F. (1970). The carbon monoxide body stores. *Ann N Y Acad Sci*, 174(1):11–22.

Coburn, R. F., Blakemore, W. S., and Forster, R. E. (1963). Endogenous carbon monoxide production in man. *J Clin Invest*, 42:1172–8.

Derbyshire, E. R. and Marletta, M. A. (2012). Structure and regulation of soluble guanylate cyclase. *Annu Rev Biochem*, 81:533–59.

Dief, A. E., Mostafa, D. K., Sharara, G. M., and Zeitoun, T. H. (2015). Hydrogen sulfide releasing naproxen offers better anti-inflammatory and chondroprotective effect relative to naproxen in a rat model of zymosan induced arthritis. *Eur Rev Med Pharmacol Sci*, 19(8):1537–46.

Feng, W., Liu, D., Feng, S., and Feng, G. (2016). Readily available fluorescent probe for carbon monoxide imaging in living cells. *Anal Chem*, 88(21):10648–10653.

Fiorucci, S., Antonelli, E., Distrutti, E., Rizzo, G., Mencarelli, A., Orlandi, S., Zanardo, R., Renga, B., Di Sante, M., Morelli, A., Cirino, G., and Wallace, J. L. (2005). Inhibition of hydrogen sulfide generation contributes to gastric injury caused by anti-inflammatory nonsteroidal drugs. *Gastroenterology*, 129(4):1210–24.

Fiorucci, S. and Distrutti, E. (2011). Coxibs, cinods and h(2)s-releasing nsaids: current perspectives in the development of safer non steroidal anti-inflammatory drugs. *Curr Med Chem*, 18(23):3494–505.

Foresti, R., Bani-Hani, M. G., and Motterlini, R. (2008). Use of carbon monoxide as a therapeutic agent: promises and challenges. *Intensive Care Med*, 34(4):649–58.

Foresti, R., Hammad, J., Clark, J. E., Johnson, T. R., Mann, B. E., Friebe, A., Green, C. J., and Motterlini, R. (2004). Vasoactive properties of corm-3, a novel water-soluble carbon monoxide-releasing molecule. *Br J Pharmacol*, 142(3):453–60.

Garcia-Gallego, S. and Bernardes, G. J. (2014). Carbon-monoxide-releasing molecules for the delivery of therapeutic co in vivo. *Angew Chem Int Ed Engl*, 53(37):9712–21.

Gilmore, T. D. (2006). Introduction to nf-kappab: players, pathways, perspectives. *Oncogene*, 25(51):6680–4.

Gonzales, M. A. and Mascharak, P. K. (2014). Photoactive metal carbonyl complexes as potential agents for targeted co delivery. *J Inorg Biochem*, 133:127–35.

Gonzales, S., Erario, M. A., and Tomaro, M. L. (2002). Heme oxygenase-1 induction and dependent increase in ferritin. a protective antioxidant stratagem in hemin-treated rat brain. *Dev Neurosci*, 24(2-3):161–8.

Greenberg, G. R. and Wintrobe, M. M. (1946). A labile iron pool. *J Biol Chem*, 165(1):397.

Gullotta, F., di Masi, A., Coletta, M., and Ascenzi, P. (2012). Co metabolism, sensing, and signaling. *Biofactors*, 38(1):1–13.

Hayden, M. S., West, A. P., and Ghosh, S. (2006). Nf-kappab and the immune response. *Oncogene*, 25(51):6758–80.

Heinemann, S. H., Hoshi, T., Westerhausen, M., and Schiller, A. (2014). Carbon monoxide–physiology, detection and controlled release. *Chem Commun (Camb)*, 50(28):3644–60.

Hentze, M. W., Muckenthaler, M. U., Galy, B., and Camaschella, C. (2010). Two to tango: regulation of mammalian iron metabolism. *Cell*, 142(1):24–38.

Herrera, B. S., Coimbra, L. S., da Silva, A. R., Teixeira, S. A., Costa, S. K., Wallace, J. L., Spolidorio, L. C., and Muscara, M. N. (2015). The h2s-releasing naproxen derivative, atb-346, inhibits alveolar bone loss and inflammation in rats with ligature-induced periodontitis. *Med Gas Res*, 5:4.

Hervera, A., Leanez, S., Motterlini, R., and Pol, O. (2013). Treatment with carbon monoxide-releasing molecules and an ho-1 inducer enhances the effects and expression of micro-opioid receptors during neuropathic pain. *Anesthesiology*, 118(5):1180–97.

Inaba, H., Fujita, K., and Ueno, T. (2015). Design of biomaterials for intracellular delivery of carbon monoxide. *Biomater Sci*.

Inguaggiato, P., Gonzalez-Michaca, L., Croatt, A. J., Haggard, J. J., Alam, J., and Nath, K. A. (2001). Cellular overexpression of heme oxygenase-1 up-regulates p21 and confers resistance to apoptosis. *Kidney Int*, 60(6):2181–91.

Ishii, T., Itoh, K., Takahashi, S., Sato, H., Yanagawa, T., Katoh, Y., Bannai, S., and Yamamoto, M. (2000). Transcription factor nrf2 coordinately regulates a group of oxidative stress-inducible genes in macrophages. *J Biol Chem*, 275(21):16023–9.

Jacobs, A. (1976). An intracellular transit iron pool. *Ciba Found Symp*, (51):91–106.

Jacobs, D., Watt, G. D., Frankel, R. B., and Papaefthymiou, G. C. (1989). Fe2+ binding to apo and holo mammalian ferritin. *Biochemistry*, 28(23):9216–21.

Johansen, D., Ytrehus, K., and Baxter, G. F. (2006). Exogenous hydrogen sulfide (h2s) protects against regional myocardial ischemia-reperfusion injury–evidence for a role of k atp channels. *Basic Res Cardiol*, 101(1):53–60.

Johnson, R. A., Kozma, F., and Colombari, E. (1999). Carbon monoxide: from toxin to endogenous modulator of cardiovascular functions. *Braz J Med Biol Res*, 32(1):1–14.

Kakhlon, O. and Cabantchik, Z. I. (2002). The labile iron pool: characterization, measurement, and participation in cellular processes(1). *Free Radic Biol Med*, 33(8):1037–46.

Katada, K., Bihari, A., Mizuguchi, S., Yoshida, N., Yoshikawa, T., Fraser, D. D., Potter, R. F., and Cepinskas, G. (2010). Carbon monoxide liberated from co-releasing molecule (corm-2) attenuates ischemia/reperfusion (i/r)-induced inflammation in the small intestine. *Inflammation*, 33(2):92–100.

Kautz, A. C., Kunz, P. C., and Janiak, C. (2016). Co-releasing molecule (corm) conjugate systems. *Dalton Trans*, 45(45):18045–18063.

Ke, B., Shen, X. D., Zhai, Y., Gao, F., Busuttil, R. W., Volk, H. D., and Kupiec-Weglinski, J. W. (2002). Heme oxygenase 1 mediates the immunomodulatory and antiapoptotic effects of interleukin 13 gene therapy in vivo and in vitro. *Hum Gene Ther*, 13(15):1845–57.

Kim, H. J., Zheng, M., Kim, S. K., Cho, J. J., Shin, C. H., Joe, Y., and Chung, H. T. (2011). Co/ho-1 induces nqo-1 expression via nrf2 activation. *Immune Netw*, 11(6):376–82.

Kohmoto, J., Nakao, A., Kaizu, T., Tsung, A., Ikeda, A., Tomiyama, K., Billiar, T. R., Choi, A. M., Murase, N., and McCurry, K. R. (2006). Low-dose carbon monoxide inhalation prevents ischemia/reperfusion injury of transplanted rat lung grafts. *Surgery*, 140(2):179–85.

Kohmoto, J., Nakao, A., Sugimoto, R., Wang, Y., Zhan, J., Ueda, H., and McCurry, K. R. (2008). Carbon monoxide-saturated preservation solution protects lung grafts from ischemia-reperfusion injury. *J Thorac Cardiovasc Surg*, 136(4):1067–75.

Kruszewski, M. (2003). Labile iron pool: the main determinant of cellular response to oxidative stress. *Mutat Res*, 531(1-2):81–92.

Kruszewski, M. (2004). The role of labile iron pool in cardiovascular diseases. *Acta Biochim Pol*, 51(2):471–80.

Lee, B. S., Heo, J., Kim, Y. M., Shim, S. M., Pae, H. O., and Chung, H. T. (2006). Carbon monoxide mediates heme oxygenase 1 induction via nrf2 activation in hepatoma cells. *Biochem Biophys Res Commun*, 343(3):965–72.

Li, Y., Wang, X., Yang, J., Xie, X., Li, M., Niu, J., Tong, L., and Tang, B. (2016). Fluorescent probe based on azobenzene-cyclopalladium for the selective imaging of endogenous carbon monoxide under hypoxia conditions. *Anal Chem*, 88(22):11154–11159.

Lo Iacono, L., Boczkowski, J., Zini, R., Salouage, I., Berdeaux, A., Motterlini, R., and Morin, D. (2011). A carbon monoxide-releasing molecule (corm-3) uncouples mitochondrial respiration and modulates the production of reactive oxygen species. *Free Radic Biol Med*, 50(11):1556–64.

Maines, M. D. (1997). The heme oxygenase system: a regulator of second messenger gases. *Annu Rev Pharmacol Toxicol*, 37:517–54.

Mann, B. E. and Motterlini, R. (2007). Co and no in medicine. *Chem Commun (Camb)*, (41):4197–208.

Marks, G. S., Brien, J. F., Nakatsu, K., and McLaughlin, B. E. (1991). Does carbon monoxide have a physiological function? *Trends Pharmacol Sci*, 12(5):185–8.

Masini, E., Vannacci, A., Failli, P., Mastroianni, R., Giannini, L., Vinci, M. C., Uliva, C., Motterlini, R., and Mannaioni, P. F. (2008). A carbon monoxide-releasing molecule (corm-3) abrogates polymorphonuclear granulocyte-induced activation of endothelial cells and mast cells. *FASEB J*, 22(9):3380–8.

Mayr, F. B., Spiel, A., Leitner, J., Marsik, C., Germann, P., Ullrich, R., Wagner, O., and Jilma, B. (2005). Effects of carbon monoxide inhalation during experimental endotoxemia in humans. *Am J Respir Crit Care Med*, 171(4):354–60.

McCoubrey, W. K., J., Huang, T. J., and Maines, M. D. (1997). Isolation and characterization of a cdna from the rat brain that encodes hemoprotein heme oxygenase-3. *Eur J Biochem*, 247(2):725–32.

McDonald, L. J. and Murad, F. (1996). Nitric oxide and cyclic gmp signaling. *Proc Soc Exp Biol Med*, 211(1):1–6.

Mede, R., Hoffmann, P., Neumann, C., Gorls, H., Schmitt, M., Popp, J., Neugebauer, U., and Westerhausen, M. (2018). Acetoxymethyl concept for intracellular administration of carbon monoxide with mn(co)3 -based photocorms. *Chemistry*, 24(13):3321–3329.

Michel, B. W., Lippert, A. R., and Chang, C. J. (2012). A reaction-based fluorescent probe for selective imaging of carbon monoxide in living cells using a palladium-mediated carbonylation. *J Am Chem Soc*, 134(38):15668–71.

Mizuguchi, S., Capretta, A., Suehiro, S., Nishiyama, N., Luke, P., Potter, R. F., Fraser, D. D., and Cepinskas, G. (2010). Carbon monoxide-releasing molecule corm-3 suppresses vascular endothelial cell sod-1/sod-2 activity while up-regulating the cell surface levels of sod-3 in a heparin-dependent manner. *Free Radic Biol Med*, 49(10):1534–41.

Moncada, S. and Higgs, E. A. (1991). Endogenous nitric oxide: physiology, pathology and clinical relevance. *Eur J Clin Invest*, 21(4):361–74.

Moncada, S., Palmer, R. M., and Higgs, E. A. (1991). Nitric oxide: physiology, pathophysiology, and pharmacology. *Pharmacol Rev*, 43(2):109–42.

Morse, D. and Choi, A. M. (2002). Heme oxygenase-1: the "emerging molecule" has arrived. *Am J Respir Cell Mol Biol*, 27(1):8–16.

Motterlini, R., Clark, J. E., Foresti, R., Sarathchandra, P., Mann, B. E., and Green, C. J. (2002). Carbon monoxide-releasing molecules: characterization of biochemical and vascular activities. *Circ Res*, 90(2):E17–24.

Motterlini, R., Gonzales, A., Foresti, R., Clark, J. E., Green, C. J., and Winslow, R. M. (1998). Heme oxygenase-1-derived carbon monoxide contributes to the suppression of acute hypertensive responses in vivo. *Circ Res*, 83(5):568–77.

Motterlini, R., Haas, B., and Foresti, R. (2012). Emerging concepts on the anti-inflammatory actions of carbon monoxide-releasing molecules (co-rms). *Med Gas Res*, 2(1):28.

Motterlini, R., Mann, B. E., and Foresti, R. (2005a). Therapeutic applications of carbon monoxide-releasing molecules. *Expert Opin Investig Drugs*, 14(11):1305–18.

Motterlini, R. and Otterbein, L. E. (2010). The therapeutic potential of carbon monoxide. *Nat Rev Drug Discov*, 9(9):728–43.

Motterlini, R., Sawle, P., Hammad, J., Bains, S., Alberto, R., Foresti, R., and Green, C. J. (2005b). Corm-a1: a new pharmacologically active carbon monoxide-releasing molecule. *FASEB J*, 19(2):284–6.

Motterlini R, Foresti R, G. C. (2002). Studies on the development of carbon monoxide-releasing molecules: potential applications for the treatment of cardiovascular dysfunction. *Carbon Monoxide and Cardiovascular Functions*, pages 249–271.

Muckenthaler, M. U., Galy, B., and Hentze, M. W. (2008). Systemic iron homeostasis and the iron-responsive element/iron-regulatory protein (ire/irp) regulatory network. *Annu Rev Nutr*, 28:197–213.

Murad, F. (1994). Regulation of cytosolic guanylyl cyclase by nitric oxide: the no-cyclic gmp signal transduction system. *Adv Pharmacol*, 26:19–33.

Mustafa, A. K., Gadalla, M. M., and Snyder, S. H. (2009). Signaling by gasotransmitters. *Sci Signal*, 2(68):re2.

Nakao, A., Faleo, G., Shimizu, H., Nakahira, K., Kohmoto, J., Sugimoto, R., Choi, A. M., McCurry, K. R., Takahashi, T., and Murase, N. (2008). Ex vivo carbon monoxide prevents cytochrome p450 degradation and ischemia/reperfusion injury of kidney grafts. *Kidney Int*, 74(8):1009–16.

Nakao, A., Huang, C. S., Stolz, D. B., Wang, Y., Franks, J. M., Tochigi, N., Billiar, T. R., Toyoda, Y., Tzeng, E., and McCurry, K. R. (2011). Ex vivo carbon monoxide delivery inhibits intimal hyperplasia in arterialized vein grafts. *Cardiovasc Res*, 89(2):457–63.

Nakao, A., Kaczorowski, D. J., Wang, Y., Cardinal, J. S., Buchholz, B. M., Sugimoto, R., Tobita, K., Lee, S., Toyoda, Y., Billiar, T. R., and McCurry, K. R. (2010). Amelioration of rat cardiac cold ischemia/reperfusion injury with inhaled hydrogen or carbon monoxide, or both. *J Heart Lung Transplant*, 29(5):544–53.

Nakao, A., Toyokawa, H., Tsung, A., Nalesnik, M. A., Stolz, D. B., Kohmoto, J., Ikeda, A., Tomiyama, K., Harada, T., Takahashi, T., Yang, R., Fink, M. P., Morita, K., Choi, A. M., and Murase, N. (2006). Ex vivo application of carbon monoxide in university of wisconsin solution to prevent intestinal cold ischemia/reperfusion injury. *Am J Transplant*, 6(10):2243–55.

Neto, J. S., Nakao, A., Kimizuka, K., Romanosky, A. J., Stolz, D. B., Uchiyama, T., Nalesnik, M. A., Otterbein, L. E., and Murase, N. (2004). Protection of transplant-induced renal ischemia-reperfusion injury with carbon monoxide. *Am J Physiol Renal Physiol*, 287(5):F979–89.

Niesel, J., Pinto, A., Peindy N'Dongo, H. W., Merz, K., Ott, I., Gust, R., and Schatzschneider, U. (2008). Photoinduced co release, cellular uptake and cytotoxicity of a tris(pyrazolyl)methane (tpm) manganese tricarbonyl complex. *Chem Commun (Camb)*, (15):1798–800.

Otterbein, L. E., Bach, F. H., Alam, J., Soares, M., Tao Lu, H., Wysk, M., Davis, R. J., Flavell, R. A., and Choi, A. M. (2000). Carbon monoxide has anti-inflammatory effects involving the mitogen-activated protein kinase pathway. *Nat Med*, 6(4):422–8.

Otterbein, L. E. and Choi, A. M. (2000). Heme oxygenase: colors of defense against cellular stress. *Am J Physiol Lung Cell Mol Physiol*, 279(6):L1029–37.

Otterbein, L. E., Kolls, J. K., Mantell, L. L., Cook, J. L., Alam, J., and Choi, A. M. (1999). Exogenous administration of heme oxygenase-1 by gene transfer provides protection against hyperoxia-induced lung injury. *J Clin Invest*, 103(7):1047–54.

Otterbein, L. E., Soares, M. P., Yamashita, K., and Bach, F. H. (2003a). Heme oxygenase-1: unleashing the protective properties of heme. *Trends Immunol*, 24(8):449–55.

Otterbein, L. E., Zuckerbraun, B. S., Haga, M., Liu, F., Song, R., Usheva, A., Stachulak, C., Bodyak, N., Smith, R. N., Csizmadia, E., Tyagi, S., Akamatsu, Y., Flavell, R. J., Billiar, T. R., Tzeng, E., Bach, F. H., Choi, A. M., and Soares, M. P. (2003b). Carbon monoxide suppresses arteriosclerotic lesions associated with chronic graft rejection and with balloon injury. *Nat Med*, 9(2):183–90.

Pacher, P., Beckman, J. S., and Liaudet, L. (2007). Nitric oxide and peroxynitrite in health and disease. *Physiol Rev*, 87(1):315–424.

Pan, T. T., Feng, Z. N., Lee, S. W., Moore, P. K., and Bian, J. S. (2006). Endogenous hydrogen sulfide contributes to the cardioprotection by metabolic inhibition preconditioning in the rat ventricular myocytes. *J Mol Cell Cardiol*, 40(1):119–30.

Pfeiffer, H., Rojas, A., Niesel, J., and Schatzschneider, U. (2009). Sonogashira and "click" reactions for the n-terminal and side-chain functionalization of peptides with [mn(co)3(tpm)]+-based co releasing molecules (tpm = tris(pyrazolyl)methane). *Dalton Trans*, (22):4292–8.

Powell, C. R., Dillon, K. M., and Matson, J. B. (2018). A review of hydrogen sulfide (h2s) donors: Chemistry and potential therapeutic applications. *Biochem Pharmacol*, 149:110–123.

Qin, W., Zhang, J., Lv, W., Wang, X., and Sun, B. (2013). Effect of carbon monoxide-releasing molecules ii-liberated co on suppressing inflammatory response in sepsis by interfering with nuclear factor kappa b activation. *PLoS One*, 8(10):e75840.

Rimmer, R. D., Pierri, A. E., and Ford, P. C. (2012). Photochemically activated carbon monoxide release for biological targets. toward developing air-stable photocorms labilized by visible light. *Coordination Chemistry Reviews*, 256(15-16):1509–1519.

Rimmer, R. D., Richter, H., and Ford, P. C. (2010). A photochemical precursor for carbon monoxide release in aerated aqueous media. *Inorg Chem*, 49(3):1180–5.

Rochette, L., Cottin, Y., Zeller, M., and Vergely, C. (2013). Carbon monoxide: mechanisms of action and potential clinical implications. *Pharmacol Ther*, 137(2):133–52.

Romanski, S. (2013). *Synthese und Evaluation geschützter oxysubstituierter Dien-Fe(CO) 3 -Komplexe als enzymatisch aktivierbare CO-freisetzende Moleküle (ET-CORMs)*. Dr. Hut.

Romanski, S., Kraus, B., Guttentag, M., Schlundt, W., Rucker, H., Adler, A., Neudorfl, J. M., Alberto, R., Amslinger, S., and Schmalz, H. G. (2012). Acyloxybutadiene tricarbonyl iron complexes as enzyme-triggered co-releasing molecules (et-corms): a structure-activity relationship study. *Dalton Trans*, 41(45):13862–75.

Romanski, S., Kraus, B., Schatzschneider, U., Neudorfl, J. M., Amslinger, S., and Schmalz, H. G. (2011a). Acyloxybutadiene iron tricarbonyl complexes as enzyme-triggered co-releasing molecules (et-corms). *Angew Chem Int Ed Engl*, 50(10):2392–6.

Romanski, S., Neudorfl, J. M., and Schmalz, H. G. (2011b). (rs)-tricarbon-yl(eta-1,3-diacet-oxy-5,5-dimethyl-cyclo-hexa-1,3-diene)iron(0). *Acta Crystallogr Sect E Struct Rep Online*, 67(Pt 11):m1530.

Romanski, S., Stamellou, E., Jaraba, J. T., Storz, D., Kramer, B. K., Hafner, M., Amslinger, S., Schmalz, H. G., and Yard, B. A. (2013). Enzyme-triggered co-releasing molecules (et-corms): Evaluation of biological activity in relation to their structure. *Free Radic Biol Med*, 65:78–88.

Romao, C. C., Blattler, W. A., Seixas, J. D., and Bernardes, G. J. (2012). Developing drug molecules for therapy with carbon monoxide. *Chem Soc Rev*, 41(9):3571–83.

Rosas, I. O., Goldberg, H. J., Collard, H. R., El-Chemaly, S., Flaherty, K., Hunninghake, G. M., Lasky, J. A., Lederer, D. J., Machado, R., Martinez, F. J., Maurer, R., Teller, D., Noth, I., Peters, E., Raghu, G., Garcia, J. G. N., and Choi, A. M. K. (2018). A phase ii clinical trial of low-dose inhaled carbon monoxide in idiopathic pulmonary fibrosis. *Chest*, 153(1):94–104.

Ryter, S. W. and Choi, A. M. (2009). Heme oxygenase-1/carbon monoxide: from metabolism to molecular therapy. *Am J Respir Cell Mol Biol*, 41(3):251–60.

Sandouka, A., Balogun, E., Foresti, R., Mann, B. E., Johnson, T. R., Tayem, Y., Green, C. J., Fuller, B., and Motterlini, R. (2005). Carbon monoxide-releasing molecules (co-rms) modulate respiration in isolated mitochondria. *Cell Mol Biol (Noisy-le-grand)*, 51(4):425–32.

Sarady, J. K., Otterbein, S. L., Liu, F., Otterbein, L. E., and Choi, A. M. (2002). Carbon monoxide modulates endotoxin-induced production of granulocyte macrophage colony-stimulating factor in macrophages. *Am J Respir Cell Mol Biol*, 27(6):739–45.

Sato, K., Balla, J., Otterbein, L., Smith, R. N., Brouard, S., Lin, Y., Csizmadia, E., Sevigny, J., Robson, S. C., Vercellotti, G., Choi, A. M., Bach, F. H., and Soares, M. P. (2001). Carbon monoxide generated by heme oxygenase-1 suppresses the rejection of mouse-to-rat cardiac transplants. *J Immunol*, 166(6):4185–94.

Sawle, P., Foresti, R., Mann, B. E., Johnson, T. R., Green, C. J., and Motterlini, R. (2005). Carbon monoxide-releasing molecules (co-rms) attenuate the inflammatory response elicited by lipopolysaccharide in raw264.7 murine macrophages. *Br J Pharmacol*, 145(6):800–10.

Schatzschneider, U. (2010). Photoactivated biological activity of transition metal complexes. *Eur. J. Inorg. Chem*, (10):1451–1467.

Schatzschneider, U. (2011). Photocorms: Light-triggered release of carbon monoxide from the coordination sphere of transition metal complexes for biological applications. *Inorganica Chimica Acta*, 374(1):19–23.

Schatzschneider, U. (2015). Novel lead structures and activation mechanisms for co-releasing molecules (corms). *Br J Pharmacol*, 172(6):1638–50.

Seldon, M. P., Silva, G., Pejanovic, N., Larsen, R., Gregoire, I. P., Filipe, J., Anrather, J., and Soares, M. P. (2007). Heme oxygenase-1 inhibits the expression of adhesion molecules associated with endothelial cell activation via inhibition of nf-kappab rela phosphorylation at serine 276. *J Immunol*, 179(11):7840–51.

Shoman, M. E., DuMond, J. F., Isbell, T. S., Crawford, J. H., Brandon, A., Honovar, J., Vitturi, D. A., White, C. R., Patel, R. P., and King, S. B. (2011). Acyloxy nitroso compounds as nitroxyl (hno) donors: kinetics, reactions with thiols, and vasodilation properties. *J Med Chem*, 54(4):1059–70.

Sitnikov, N. S., Li, Y., Zhang, D., Yard, B., and Schmalz, H. G. (2015). Design, synthesis, and functional evaluation of co-releasing molecules triggered by penicillin g amidase as a model protease. *Angew Chem Int Ed Engl*.

Sjostrand, T. (1951). Endogenous formation of carbon monoxide; the co concentration in the inspired and expired air of hospital patients. *Acta Physiol Scand*, 22(2-3):137–41.

Sjostrand, T. (1952a). The formation of carbon monoxide by in vitro decomposition of haemoglobin in bile pigments. *Acta Physiol Scand*, 26(4):328–33.

Sjostrand, T. (1952b). The in vitro formation of carbon monoxide in blood. *Acta Physiol Scand*, 24(4):314–32.

Sodha, N. R., Clements, R. T., Feng, J., Liu, Y., Bianchi, C., Horvath, E. M., Szabo, C., Stahl, G. L., and Sellke, F. W. (2009). Hydrogen sulfide therapy attenuates the inflammatory response in a porcine model of myocardial ischemia/reperfusion injury. *J Thorac Cardiovasc Surg*, 138(4):977–84.

Sodha, N. R. and Sellke, F. W. (2015). Attenuation of inflammatory responses by hydrogen sulfide (h(2)s) in ischemia/reperfusion injury. *Methods Enzymol*, 555:127–44.

Song, H., Bergstrasser, C., Rafat, N., Hoger, S., Schmidt, M., Endres, N., Goebeler, M., Hillebrands, J. L., Brigelius-Flohe, R., Banning, A., Beck, G., Loesel, R., and Yard, B. A. (2009). The carbon monoxide releasing molecule (corm-3) inhibits expression of vascular cell adhesion molecule-1 and e-selectin independently of haem oxygenase-1 expression. *Br J Pharmacol*, 157(5):769–80.

Song, H., Hoeger, S., Hillebrands, J. L., Mandel, I., Loesel, R., Beck, G., Schilling, L., Schnuelle, P., and Yard, B. (2010). Corms protect endothelial cells during cold preservation, resulting in inhibition of intimal hyperplasia after aorta transplantation in rats. *Transpl Int*, 23(11):1144–53.

Song, R., Kubo, M., Morse, D., Zhou, Z., Zhang, X., Dauber, J. H., Fabisiak, J., Alber, S. M., Watkins, S. C., Zuckerbraun, B. S., Otterbein, L. E., Ning, W., Oury, T. D., Lee, P. J., McCurry, K. R., and Choi, A. M. (2003). Carbon monoxide induces cytoprotection in rat orthotopic lung transplantation via anti-inflammatory and anti-apoptotic effects. *Am J Pathol*, 163(1):231–42.

Stamellou, E., Storz, D., Botov, S., Ntasis, E., Wedel, J., Sollazzo, S., Kramer, B. K., van Son, W., Seelen, M., Schmalz, H. G., Schmidt, A., Hafner, M., and Yard, B. A. (2014). Different design of enzyme-triggered co-releasing molecules (et-corms) reveals quantitative differences in biological activities in terms of toxicity and inflammation. *Redox Biol*, 2:739–48.

Steiger, C., Uchiyama, K., Takagi, T., Mizushima, K., Higashimura, Y., Gutmann, M., Hermann, C., Botov, S., Schmalz, H. G., Naito, Y., and Meinel, L. (2016). Prevention of colitis by controlled oral drug delivery of carbon monoxide. *J Control Release*, 239:128–36.

Stupfel, M. and Bouley, G. (1970). Physiological and biochemical effects on rats and mice exposed to small concentrations of carbon monoxide for long periods. *Ann N Y Acad Sci*, 174(1):342–68.

Suematsu, M., Goda, N., Sano, T., Kashiwagi, S., Egawa, T., Shinoda, Y., and Ishimura, Y. (1995). Carbon monoxide: an endogenous modulator of sinusoidal tone in the perfused rat liver. *J Clin Invest*, 96(5):2431–7.

Suematsu, M., Kashiwagi, S., Sano, T., Goda, N., Shinoda, Y., and Ishimura, Y. (1994). Carbon monoxide as an endogenous modulator of hepatic vascular perfusion. *Biochem Biophys Res Commun*, 205(2):1333–7.

Szabo, C. (2007). Hydrogen sulphide and its therapeutic potential. *Nat Rev Drug Discov*, 6(11):917–35.

Takagi, T., Uchiyama, K., and Naito, Y. (2015). The therapeutic potential of carbon monoxide for inflammatory bowel disease. *Digestion*, 91(1):13–8.

Takahashi, K., Tamagawa, S., Sakano, H., Katagi, T., and Mizuno, N. (1995). Effects of the ester moiety on stereoselective hydrolysis of several propranolol prodrugs in rat tissues. *Biol Pharm Bull*, 18(10):1401–4.

Tenhunen, R., Marver, H. S., and Schmid, R. (1968). The enzymatic conversion of heme to bilirubin by microsomal heme oxygenase. *Proc Natl Acad Sci U S A*, 61(2):748–55.

Toombs, C. F., Insko, M. A., Wintner, E. A., Deckwerth, T. L., Usansky, H., Jamil, K., Goldstein, B., Cooreman, M., and Szabo, C. (2010). Detection of exhaled hydrogen sulphide gas in healthy human volunteers during intravenous administration of sodium sulphide. *Br J Clin Pharmacol*, 69(6):626–36.

Tsui, T. Y., Obed, A., Siu, Y. T., Yet, S. F., Prantl, L., Schlitt, H. J., and Fan, S. T. (2007). Carbon monoxide inhalation rescues mice from fulminant hepatitis through improving hepatic energy metabolism. *Shock*, 27(2):165–71.

Tsui, T. Y., Siu, Y. T., Schlitt, H. J., and Fan, S. T. (2005). Heme oxygenase-1-derived carbon monoxide stimulates adenosine triphosphate generation in human hepatocyte. *Biochem Biophys Res Commun*, 336(3):898–902.

Vadori, M., Seveso, M., Besenzon, F., Bosio, E., Tognato, E., Fante, F., Boldrin, M., Gavasso, S., Ravarotto, L., Mann, B. E., Simioni, P., Ancona, E., Motterlini, R., and Cozzi, E. (2009). In vitro and in vivo effects of the carbon monoxide-releasing molecule, corm-3, in the xenogeneic pig-to-primate context. *Xenotransplantation*, 16(2):99–114.

Wagener, F. A., Volk, H. D., Willis, D., Abraham, N. G., Soares, M. P., Adema, G. J., and Figdor, C. G. (2003). Different faces of the heme-heme oxygenase system in inflammation. *Pharmacol Rev*, 55(3):551–71.

Wallace, J. L., Caliendo, G., Santagada, V., and Cirino, G. (2010). Markedly reduced toxicity of a hydrogen sulphide-releasing derivative of naproxen (atb-346). *Br J Pharmacol*, 159(6):1236–46.

Wallace, J. L., Caliendo, G., Santagada, V., Cirino, G., and Fiorucci, S. (2007). Gastrointestinal safety and anti-inflammatory effects of a hydrogen sulfide-releasing diclofenac derivative in the rat. *Gastroenterology*, 132(1):261–71.

Wang, J., Karpus, J., Zhao, B. S., Luo, Z., Chen, P. R., and He, C. (2012). A selective fluorescent probe for carbon monoxide imaging in living cells. *Angew Chem Int Ed Engl*, 51(38):9652–6.

Wang, R. (2002). Two's company, three's a crowd: can h2s be the third endogenous gaseous transmitter? *FASEB J*, 16(13):1792–8.

Wang, R. (2014). Gasotransmitters: growing pains and joys. *Trends Biochem Sci*, 39(5):227–32.

Wang, R., Wang, Z., and Wu, L. (1997). Carbon monoxide-induced vasorelaxation and the underlying mechanisms. *Br J Pharmacol*, 121(5):927–34.

White, W. B., Schnitzer, T. J., Bakris, G. L., Frayssinet, H., Duquesroix, B., and Weber, M. (2011). Effects of naproxcinod on blood pressure in patients with osteoarthritis. *Am J Cardiol*, 107(9):1338–45.

Wu, L. and Wang, R. (2005). Carbon monoxide: endogenous production, physiological functions, and pharmacological applications. *Pharmacol Rev*, 57(4):585–630.

Yabluchanskiy, A., Sawle, P., Homer-Vanniasinkam, S., Green, C. J., Foresti, R., and Motterlini, R. (2012). Corm-3, a carbon monoxide-releasing molecule, alters the inflammatory response and reduces brain damage in a rat model of hemorrhagic stroke. *Crit Care Med*, 40(2):544–52.

Yang, L., Quan, S., and Abraham, N. G. (1999). Retrovirus-mediated ho gene transfer into endothelial cells protects against oxidant-induced injury. *Am J Physiol*, 277(1 Pt 1):L127–33.

Zanardo, R. C., Brancaleone, V., Distrutti, E., Fiorucci, S., Cirino, G., and Wallace, J. L. (2006). Hydrogen sulfide is an endogenous modulator of leukocyte-mediated inflammation. *FASEB J*, 20(12):2118–20.

Zobi, F. (2013). Co and co-releasing molecules in medicinal chemistry. *Future Med Chem*, 5(2):175–88.

Zobi, F., Quaroni, L., Santoro, G., Zlateva, T., Blacque, O., Sarafimov, B., Schaub, M. C., and Bogdanova, A. Y. (2013). Live-fibroblast ir imaging of a cytoprotective photocorm activated with visible light. *J Med Chem*, 56(17):6719–31.

Zuckerbraun, B. S., Chin, B. Y., Bilban, M., d'Avila, J. C., Rao, J., Billiar, T. R., and Otterbein, L. E. (2007). Carbon monoxide signals via inhibition of cytochrome c oxidase and generation of mitochondrial reactive oxygen species. *FASEB J*, 21(4):1099–106.

Zuckerbraun, B. S., Chin, B. Y., Wegiel, B., Billiar, T. R., Czsimadia, E., Rao, J., Shimoda, L., Ifedigbo, E., Kanno, S., and Otterbein, L. E. (2006). Carbon monoxide reverses established pulmonary hypertension. *J Exp Med*, 203(9):2109–19.

Curriculum Vitae

Personal information

Name:	Dennis Erich Storz
Date of birth:	March 22nd 1986
Place of birth:	Villingen-Schwenningen, Baden-Württemberg
Marital status:	Single
Father:	Klaus Storz
Mother:	Angelika Kayan

Education

1996 – 2005	Highschool, Gymnasium am Hoptbühl, Villingen-Schwenningen (Abitur degree)

Social service

2005 – 2006	Civil Service, Nachsorgeklinik Tannheim
2007 – 2012	Voluntary Year of Social Service (FSJ) and Emergency Medical Assistant, Deutsches Rotes Kreuz Rettungsdienst Schwarzwald-Baar gGmbH

Academic education

2008 – 2015	Studies of Human Medicine, Medical Faculty Mannheim, Heidelberg University
10.09.2015	Medical Approbation
2012 – 2018	Doctoral Candidate, Vth Medical Department of Nephrology, Endocrinology and Rheumatology, Medical Faculty Mannheim, Heidelberg University

Professional career

2015	Lecturer at Heilpraktikerakademie Wong, Bad Dürkheim
2016 – 2018	Resident at Düsseldorf University Hospital, Department of General Paediatrics, Neonatology and Paedatric Cardiology
Sept. 2018 to present	Professional Diploma in Tropical Medicine and Hygiene at the London School of Hygiene and Tropical Medicine, United Kingdom

Publications

Peer-reviewed journal articles

Different design of enzyme-triggered CO-releasing molecules (ET-CORMs) reveals quantitative differences in biological activities in terms of toxicity and inflammation.
Stamellou, E.*, Storz, D.*, Botov, S., Ntasis, E., Wedel, J., Sollazzo, S., Krämer, B.K., van Son, W., Seelen, M., Schmalz, H.G., Schmidt, A., Hafner, M., Yard, B.A. (2014). Redox Biology 2: 739-748.
**SE and SD have contributed equally to this study*

Enzyme-triggered CO-releasing molecules (ET-CORMs): Evaluation of biological activity in relation to their structure.
Romanski, S., Stamellou, E., Jaraba, J.T., Storz, D., Krämer, B.K., Hafner, M., Amslinger, S., Schmalz, H.G., Yard, B.A. (2013). Free Radical Biology and Medicine 65: 78-88.

Case reports

Atypical neuroimaging in Wilson's disease.
Patell, R., Dosi, R., Joshi, H.K., Storz, D. (2014). British Medical Journal Case Reports. (doi:10.1136/bcr-2013-200100).

Conference contributions

Fever and sacroiliac pain: Think systemic brucellosis!
Winkler, W., Storz, D., Bartelt, J., Urffer, S., Tarr, P.
83. Schweizerische Gesellschaft für Allgemeine Innere Medizin - Jahresversammlung, Basel, Schweiz (2015).

Splenomegalie, Ösophagusvarizen, Panzytopenie und Koagulopathie - Komplizierter M. Gaucher oder einfache Pfortaderthrombose?
Storz, D., Thimm, E., Welsch, S., Schaper, J., Esposito, I., Friedt, M.
32. Jahrestagung der Gesellschaft für pädiatrische Gastroenterologie und Ernährung, Alpbach, Österreich (2017).

Acknowledgements

Ich bedanke mich bei Herrn Prof. Dr. rer. nat. Benito A. Yard für die Betreuung bei dieser Arbeit und die Möglichkeit sie in einem sehr entspannten, gleichzeitig fokussierten und zielstrebigen Umfeld zu bearbeiten.

Besonderer Dank gilt meiner Betreuerin Eleni Stamellou für die Hilfsbereitschaft, Unterstützung und Geduld, die mir so häufig entgegenbracht wurde. Ich danke für die vielen Gespräche auf wissenschaftlicher und persönlicher Ebene, sowie für die wichtigen Diskussionen, die mir zum tieferen Verständnis der Thematik verhalfen.

Ich danke der gesamten Forschungsgruppe für die Unterstützung während den Experimenten, die von allen als selbstverständlich angesehen wurde. Im Einzelnen möchte ich Frau Annette Breedijk, Frau Katharina Prem und Frau Sophie Gärtner besonders für die große technische Hilfsbereitschaft im Labor danken.

Mein Dank gilt ebenso den wissenschaftlichen Kollegen Prama Pallavi, Johannes Wedel und Emmanouil Ntasis für den bereichernden, konstruktiven Austausch und die angenehme Zusammenarbeit.

Auch über die wissenschaftliche Arbeit hinaus danke ich meinen engsten Freunden für die endlose moralische Unterstützung und den Rückenwind. Ausdrücklich danke ich dabei Mathias Davids, der mich gerade gegen Ende insbesondere fachlich und technisch unterstütz hat, dieser Dissertation den letzten Schliff zu geben.

Außerdem danke ich meiner Familie für ihr großes Verständnis während der gesamten Arbeit und besonders Kim und Moaz Bajwa für das detaillierte Korrekturlesen. Zu guter Letzt danke ich meiner Mutter Angelika Kayan, meinem Vater Klaus Storz und meinem Stiefvater Günter Kayan für ihren unverzichtbaren, nie endenden Rückhalt.